New insights on the Green River petroleum system in the Uinta basin from hydrous pyrolysis experiments

Tim E. Ruble, M. D. Lewan, and R. P. Philp

ABSTRACT

The Tertiary Green River petroleum system in the Uinta basin generated about 500 million bbl of recoverable, high pour-point, paraffinic crude oil from lacustrine source rocks. A prolific complex of marginal and open-lacustrine source rocks, dominated by carbonate oil shales containing up to 60 wt. % type I kerogen, occur within distinct stratigraphic units in the basin. Petroleum generation is interpreted to originate from source pods in the basal Green River Formation buried to depths greater than 3000 m along the steeply dipping northern margin of the basin. Producing fields in the Altamont-Bluebell trend have elevated pore-fluid pressures approaching 80% of lithostatic pressure and are completed in strata where open fractures provide permeability. Active hydrocarbon generation is one explanation for the origin of the overpressured reservoirs.

In this study, experiments were undertaken to examine the mechanisms of hydrocarbon generation and accumulation in the Uinta basin. We combined analyses of representative source rocks from the entire Green River stratigraphic section with detailed laboratory simulation experiments using both open- and closed-system pyrolysis. This information provides new insights on lacustrine source rock lithofacies, gas–oil–source rock correlations, hydrocarbon generation kinetics, and basin modeling. The results show that the basal Green River Formation contains a unique type I source facies responsible for generation of paraffinic crude oils. The classic type I oil shales in the upper Green River Formation correlate well with low-maturity aromatic-asphaltic samples. We determined kinetic parameters for the source rocks and used them to develop basin models for hydrocarbon generation. The models show that hydrous pyrolysis kinetic parameters are more consistent with the natural data in terms of predicted timing and extent of oil generation as compared to models using Rock-Eval kinetics.

Manuscript received May 6, 1999; revised manuscript received August 7, 2000; final acceptance October 10, 2000.

AUTHORS

TIM E. RUBLE ~ *CSIRO Division of Petroleum Resources, Box 136, North Ryde, NSW, 1670, Australia; tim.ruble@syd.dpr.csiro.au*

Tim Ruble is a research scientist at CSIRO Petroleum in Sydney, Australia, and is currently undertaking organic geochemical studies on kinetics of hydrocarbon generation, hydrocarbon-bearing fluid inclusions, and lacustrine petroleum systems. He received a B.S. degree from Truman State University (1987) and an M.S. degree from the University of Oklahoma (1990). He obtained his Ph.D. from the University of Oklahoma (1996) for research into the mechanisms of oil generation in the Uinta basin, Utah. During the course of his studies, he was employed as an intern with Mobil Oil both in their research labs (1990) and in an exploration unit (1991). In 1995, he was employed with the U.S. Geological Survey in Denver, Colorado, and participated in a geochemical study of the Dnieper-Donets basin, Ukraine. In 1996 he joined CSIRO and has been actively involved in a variety of research and contract projects using the analysis of hydrocarbons trapped within fluid inclusions.

M. D. LEWAN ~ *U.S. Geological Survey, Box 25046, MS 977, Denver, Colorado, 80225; mlewan@usgs.gov*

Michael D. Lewan is an organic geochemist and petroleum geologist for the Central Energy Team of the U.S. Geological Survey. He has 13 years' experience with Amoco Production Co. as a research scientist in their Tulsa Research Center and 3 years experience with Shell Oil Co. as an exploration geologist in their New Orleans Offshore E&P Office. He has pioneered the development of hydrous pyrolysis in simulating natural petroleum formation, which has been used to evaluate expulsion, kinetic parameters, and quality of petroleum formed from various source rocks containing different types of organic matter. He is the recipient of the Organic Geochemistry Division of the Geochemical Society 1985 Best Paper Award and the AAPG 1991 George C. Matson Memorial Award for Best Paper and was an AAPG 1992 Distinguished Lecturer. He has a Ph.D. from

the University of Cincinnati and an M.S. degree from Michigan Technology University.

R. P. PHILP ~ *University of Oklahoma, School of Geology and Geophysics, 100 E. Boyd Street, Norman, Oklahoma, 73019; pphilp@ou.edu*

R. Paul Philp is currently professor of petroleum and environmental geochemistry in the School of Geology and Geophysics at the University of Oklahoma. He received his Ph.D. from the University of Sydney, Australia, and more recently received his D.Sc. degree from the same university. His current research interests are focused on petroleum, environmental, and forensic geochemistry, with an emphasis on molecular and isotopic characterization of oils, gases, rock extracts, and contaminants for the purposes of source determination; characterization of depositional environments, maturity, and biodegradation; and correlation. He has published more than 240 articles in national and international journals and has lectured extensively on various aspects of geochemistry around the world.

ACKNOWLEDGEMENTS

Financial support for this research was provided in part by the U.S. Geological Survey Volunteers for Science program (M. D. Lewan and Janet K. Pitman) and by a research assistantship sponsored by Phillips Petroleum. We gratefully acknowledge the assistance of Jon Allen, Donald E. Anders, Brian J. Cardott, Jerry L. Clayton, Ted A. Daws, Thomas D. Fouch, Dick Gibson, Daniel M. Jarvie, J. David King, Martin Koopmans, Paul G. Lillis, S. Mark Monk, Vito F. Nuccio, James G. Palacas, Mark J. Pawlewicz, Eleanora I. Robbins, Charles N. Threlkeld, and Augusta Warden. We also thank Kevin Bohacs, Ken Peters, Neil Sherwood, and Jerry J. Sweeney for the significant time they spent reviewing this manuscript and for their very helpful suggestions.

INTRODUCTION

The Tertiary Green River petroleum system in the Uinta basin of northeastern Utah has historically received considerable attention as a classic model for lacustrine source rock deposition (e.g., Bradley, 1931; Dane, 1954, 1955; Picard, 1955, 1957, 1959; Ray et al., 1956; Abbott, 1957; Cashion, 1957; Picard et al., 1973; Cashion and Donnell, 1974; Fouch 1975, 1976, 1981; Fouch et al., 1976, 1992; Ryder et al., 1976; Dyni et al., 1985; Weiss et al., 1990; Remy, 1992; Wiggins and Harris, 1994) and as a model for hydrocarbon generation from these types of source facies (e.g., Sweeney et al., 1987; Anders et al., 1992; Bredehoeft et al., 1994; Fouch et al., 1994; McPherson, 1996; Ruble, 1996). Many articles characterize organic components from Green River shale extracts (e.g., Robinson et al., 1965; Robinson, 1969; Anders and Robinson, 1971, 1973; Anders et al., 1975; Robinson and Cook, 1975; Anders and Gerrild, 1984). In contrast, few articles use modern geochemical methods of analyses to correlate the crude oils and gases in the basin with their respective source rocks (e.g., Philippi, 1974; Anders et al., 1992; Hatcher et al., 1992; Rice et al., 1992; Ruble, 1996; Mueller, 1998).

In 1972, Reed and Henderson examined a wide variety of Uinta basin crude oils for alkane and elemental composition and proposed that stratigraphy controls the composition of the crude oils and that the oil shales are not the dominant source rocks of the reservoired petroleum. A classic oil–source rock correlation study for the Uinta basin used various geochemical analyses, including biomarkers, to associate the major waxy crude oil production with source rocks from the basal Green River Formation and to correlate minor occurrences of shallow low-maturity oil with upper units in this formation (Tissot et al., 1978). Similar conclusions were reached by Fouch et al. (1994) who presented a comprehensive examination of the Uinta basin Green River petroleum system and integrated all available source rock, crude oil, and natural gas data with new geological information.

Fouch et al. (1994) also generated basin models of the Green River petroleum system. This work extended a classic study published by Sweeney et al. (1987), which was the first of many to use nonisothermal open-system kinetic parameters derived from Green River oil shales to model hydrocarbon generation from lacustrine source rocks. Such open-system kinetic parameters were developed during studies of the retorting mechanisms for petroleum generation from oil shales (e.g., Braun and Rothman, 1975; Campbell et al., 1978; Shih and Sohn, 1980; Burnham et al., 1987; Sweeney, 1988). Recent studies also used open-system kinetic parameters to develop more sophisticated three-dimensional models of oil generation and migration in the Uinta basin (Bredehoeft et al., 1994; McPherson, 1996). An important conclusion from these modeling studies is that the Uinta basin is currently an active petroleum system and that oil and gas generation are responsible for high pore-fluid pressures in the deeply buried reservoirs of the Altamont-Bluebell field.

One of the difficulties with most of the previous oil–source rock correlation studies in the Uinta basin has been the lack of sufficient samples or detailed biomarker analyses to differentiate source characteristics from maturity effects. Tissot et al. (1978) attempted to overcome this problem by using a wide range of natural samples, but complex lacustrine facies variations obscure maturity relationships and raise serious questions regarding the validity of their maturation series. A useful method to overcome facies variability has been to use artificial maturation experiments to examine compositional variations in pyrolysates from the Green River shale (e.g., Evans and Felbeck, 1983). Unfortunately, these studies focused solely on one facies of the Green River Formation, the mahogany zone of the Parachute Creek Member. This has also been a limitation of previous basin modeling studies because kinetic parameters for the rich oil shales of the mahogany zone are routinely applied throughout the source rock sequence, despite significant compositional differences between the source facies in stratigraphic units of the Green River Formation (Ruble, 1996; Mueller, 1998; Ruble and Philp, 1998).

The objectives of our investigation are twofold: (1) define the source facies in the Green River Formation that are responsible for the discovered petroleum accumulations, and (2) evaluate the timing and extent of petroleum generation from these source facies based on different laboratory pyrolysis methods as constrained by available geological and geochemical data. Our study relies on hydrous pyrolysis, an experimental technique that simulates maturation, generation, and expulsion of oil that is physically and chemically similar to natural crude oils (Lewan et al., 1979; Lewan, 1985, 1993, 1994, 1997). We completed a maturation series of hydrous pyrolysis experiments using two thermally immature source facies (mahogany shale and lower black shale facies) that appear to represent end members of a continuum of type I kerogens from different stratigraphic levels of the Green River Formation. In addition, we conducted a limited number of hydrous pyrolysis experiments on source rocks from several different depositional units within the upper and lower black shale facies of the Green River Formation. The immiscible oils generated by these experiments were compared to a suite of four natural crude oils from different stratigraphic horizons thought to be representative of the various types of crude oils in the Uinta basin. Comparison of the pyrolysates to other samples, including additional Uinta basin crude oils and natural gases, has also been undertaken using previously published geochemical information. Hydrous pyrolysis experiments on the two main source facies (mahogany shale and lower black shale facies) have been conducted at various times and temperatures to determine isothermal kinetic parameters for immiscible oil generation. These data were compared to open-system Rock-Eval kinetic parameters determined on aliquots of the same samples. The kinetic parameters determined by these two methods were incorporated into a revised 1-D basin model for the Altamont field to assess differences in the timing and extent of oil generation, with emphasis on active petroleum generation as a possible mechanism for the formation of overpressures.

To effectively address our objectives, this article is divided into four major sections: (1) designation of the various source facies and the geological settings in which they occur, (2) description of the experimental approach and organic phases produced during laboratory simulation of natural maturation, (3) petroleum composition and correlations that distinguish the probable source facies, and (4) timing and extent of petroleum generation as predicted by different kinetic models. Collectively, these sections provide important new insights on the origin, timing, and extent of petroleum generation in the Uinta basin, and the results may serve as a useful analog for lacustrine petroleum systems worldwide.

SOURCE ROCKS

The Green River depositional system involves two early Tertiary lakes: Lake Uinta in the Uinta-Piceance basin of northwestern Colorado and northeastern Utah and Lake Gosiute in the greater Green River basin of northwestern Colorado and southwestern Wyoming (Figure 1). The greater Uinta-Piceance basin is commonly subdivided into the Uinta basin to the west of the Douglas Creek arch and the Piceance basin to the east. This investigation focuses on the Uinta basin, where the lacustrine source rocks of the Green River Formation are buried to sufficient depths for oil generation.

The Uinta basin encompasses an area of approximately 24,000 km^2 (Osmond, 1964) and is both a topographic and structural trough filled by as much as 5000 m of Late Cretaceous to early Oligocene lacustrine and fluvial sedimentary rocks (Johnson, 1985). The Uinta basin is a sharply asymmetrical continental intermontane basin that has a steep north flank and is

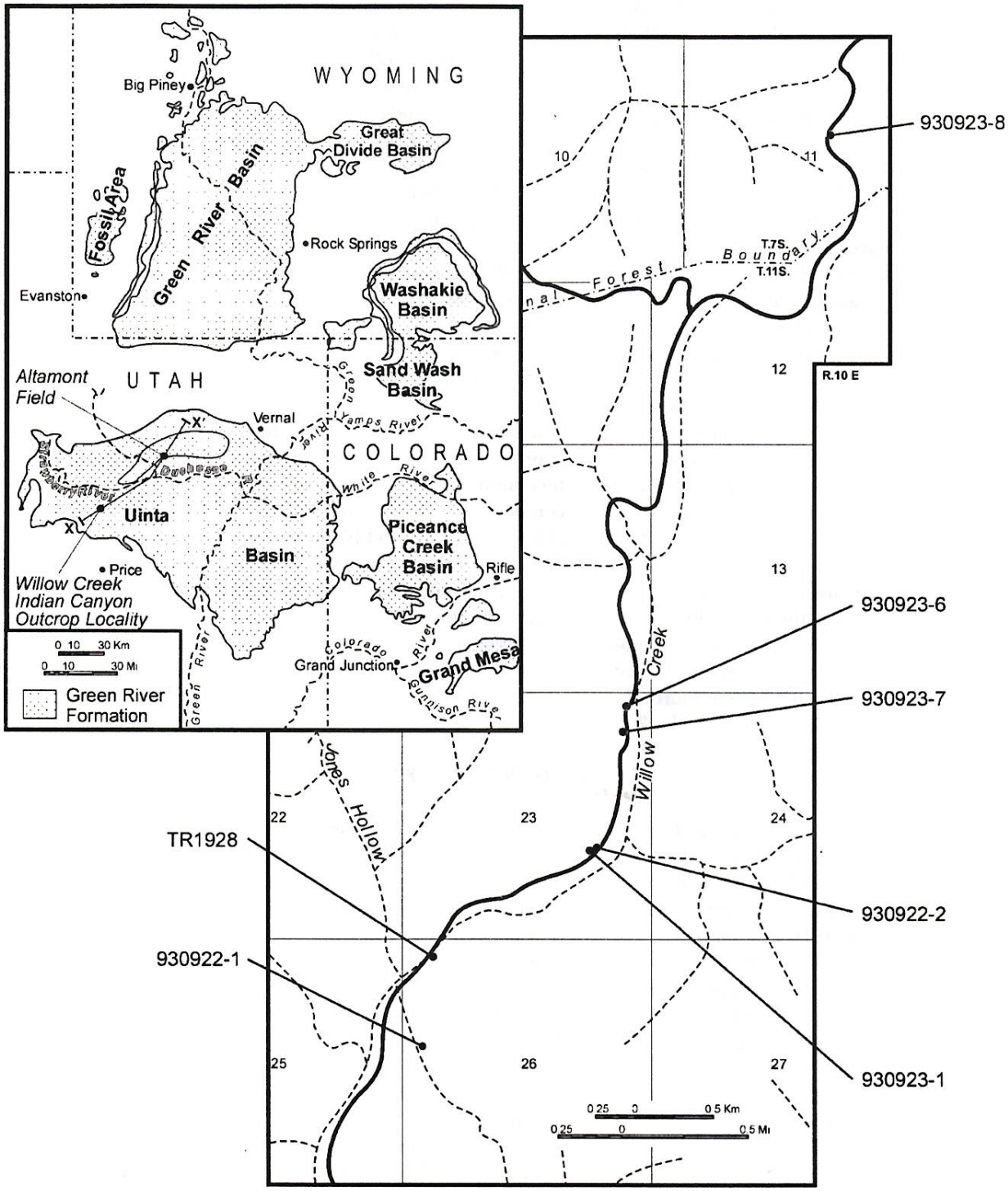

Figure 1. Regional base map of Tertiary lacustrine basins (top left) showing the locations of the Willow Creek–Indian Canyon outcrop locality and the Altamont oil/gas field in the western Uinta basin (modified from Robinson, 1969). The location of the cross section shown in Figure 2 is illustrated by line XX'. The detailed map (right) shows locations for outcrop samples identified in Table 1.

surrounded by positive structural elements: on the north by the Uinta Mountains; on the west by the Wasatch Mountains; on the south by the Uncompahgre and San Rafael uplifts and the Book Cliffs erosional scarp; and on the east by the Douglas Creek arch (Abbott, 1957). Figure 2 is a generalized stratigraphic cross section illustrating the location and orientation of formations of interest to this study (Table 1).

During the Late Cretaceous the Uinta basin area was covered by an extensive sea that extended over much of the Rocky Mountain region (Abbott, 1957). When the sea withdrew because of uplifts to the west, thick Cretaceous marine shales (Mancos formation) gradually gave way to paludal and inland flood-plain deposits of shale, sandstone, and coal (Mesaverde Formation), overlain by coarse clastic continental facies (Currant Creek, North Horn, Colton, and Wasatch formations) at the beginning of the Tertiary (Burger, 1963). As the highlands rose, sedimentation partitioned within the foreland into abruptly subsiding, internally drained, intermontane basins (Franczyk et al., 1989). Coalescence of several small, freshwater lakes (notably Lake Uinta and Lake Flagstaff) in the western part of the Uinta basin ushered in a major period of Tertiary lacustrine deposition (Green River Formation) in this region (Fouch, 1976). This period was characterized by many fluctuations in lake size, resulting in complex intertonguing of lacustrine and fluvial sediments. At its maximum extent during middle Eocene Parachute Creek Member deposition, Lake Uinta expanded over the Douglas Creek arch to connect with the Piceance basin to the east and was probably contiguous with Lake Gosiute to the north (Porter, 1963). The lake became progressively more saline until by late Paleocene it developed a stratified anoxic bottom layer conducive to the preservation of organic-rich oil shales (Hunt, 1963; Johnson, 1985). In its final stage, Lake Uinta regressed into the west-central region of the basin and became hypersaline, resulting in the deposition of an unusual assemblage of evaporitic minerals (Dyni et al., 1985). Eventually the lake was filled in with coarse-grained sandstones and conglomerates (Uinta and Duchesne River formations, Bishop Conglomerate) during fluvial and alluvial deposition in the late Eocene to Oligocene or Miocene (Abbott, 1957; Untermann and Untermann, 1968).

The most important Tertiary source rocks in the Uinta basin are kerogen-rich calcareous shales and marlstones deposited as open-lacustrine facies of the Green River Formation (Fouch et al., 1994). These beds grade laterally into time-stratigraphic equivalent marginal lacustrine and fluvial/alluvial deposits in the Wasatch, Colton, and North Horn formations. To properly interpret the oil–source rock relationships in the Uinta basin, it is important to define the various source facies within the Green River petroleum system.

Offshore Open-Lacustrine Facies

The offshore open-lacustrine facies occupies the most distal position of lacustrine deposition and is where most of the Uinta basin's oil shale formed (Figure 3). The characteristic lithology of this unit is an organic-rich (type I kerogen), light brown to black, thinly laminated to very thinly bedded, mud-supported carbonate and/or calcareous claystone (Ryder et al., 1976). The carbonate component of the oil shale is composed primarily of calcite, but dolomite is also a common and diagnostic constituent (Picard et al., 1973). Interbedded within these laminated marlstones are very fine grained calcareous sandstones, siltstones, carbonate packstones, and bedded cherts (Ryder et al., 1976). Disseminated authigenic nahcolite also occurs within the oil shales as nodules, crystalline aggregates, and single crystals (Cole, 1984). The dominant fossils are algae (Cyanophyceae and Chlorophyceae), bacteria, fungi, pollen, insect fragments/pupae (Bradley, 1931), and nonmarine ostracodes (Ryder et al., 1976).

The offshore open-lacustrine oil shales were originally interpreted to have formed in a large, deep, perennial, meromictic, alkaline lake (Bradley, 1931). Although an alternative playa-lake model was proposed for oil shale deposition in the Green River basin of Wyoming (Eugster and Surdam, 1973; Eugster and Hardie, 1975; Surdam and Wolfbauer, 1975), overwhelming sedimentological and geochemical evidence support the meromictic-lake model in the Uinta and Piceance Creek basins (Desborough, 1978; Boyer, 1982; Cole, 1984). In the meromictic model, a chemocline separated the lake waters into two distinct layers: (1) an upper mixolimnion that had fresh to slightly alkaline water, ample nutrients, and sunlight, resulting in high biological activity (primarily blue-green algae); and (2) a lower monimolimnion characterized by dense, anoxic, saline, high-pH water where biological activity was restricted to anaerobic bacteria (Cole, 1984). The organic-rich laminated oil shales originated as alternating layers of bacterial/algal ooze and algae-generated low-Mg calcite in quiet water at depths from about 5 to 30 m (Ryder et al., 1976). Further details

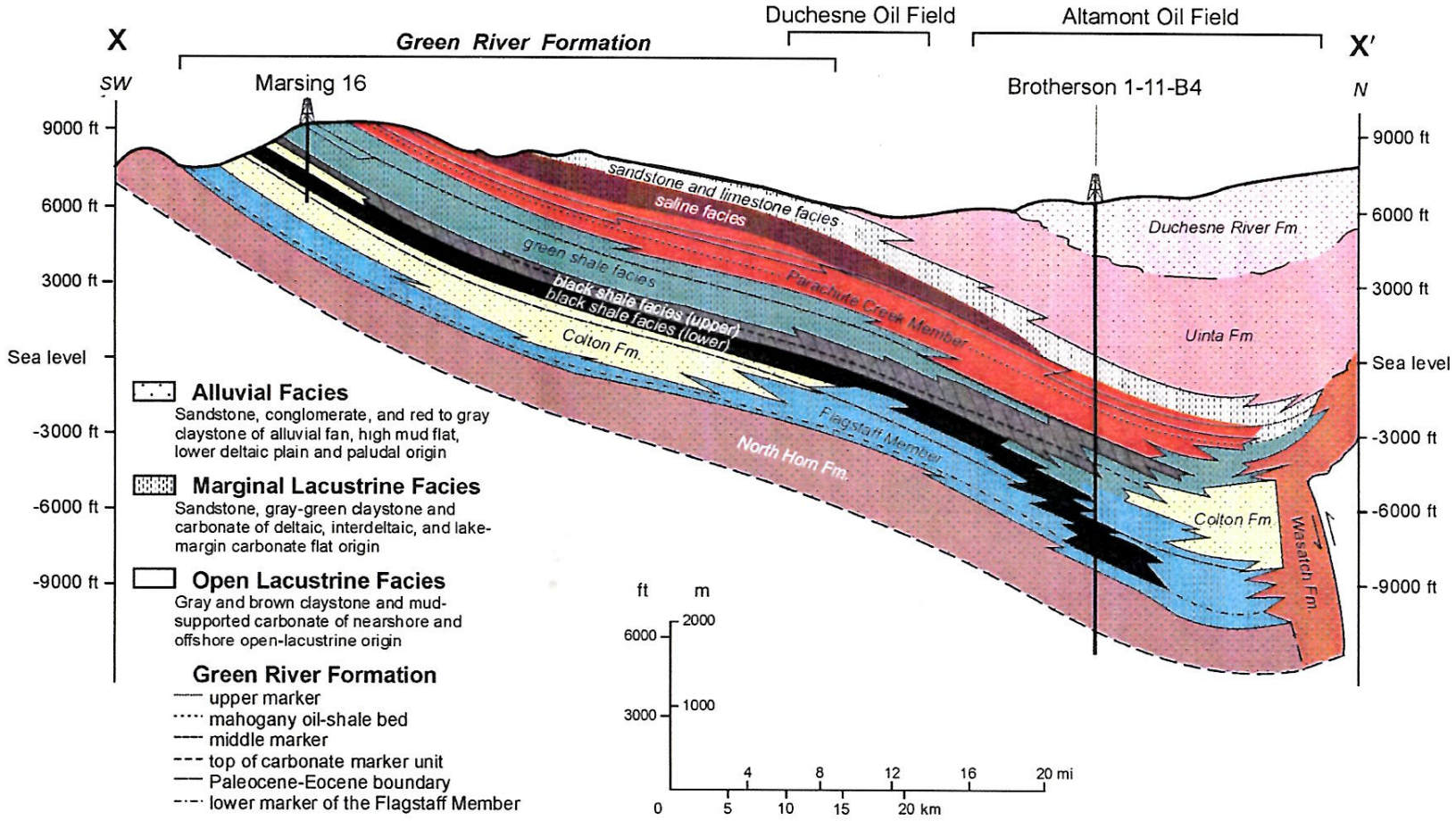

Figure 2. Generalized structural and stratigraphic cross section from outcrops along the southwest flank of the Uinta basin, through Duchesne and Altamont oil/gas fields, to the north-central part of the basin (XX′; Figure 1). Stratigraphic designations used in this investigation are shown along with generalized facies designations (modified from Fouch, 1975). Further details regarding the stratigraphic designations are in Ruble and Philp (1998).

Table 1. Sample Identifications, Locations, and Rock-Eval Data for the Outcrop Source Rocks Used in This Investigation

Sample Number	Stratigraphic Unit	Source Facies Type	Location	Sample Characteristics	% EOM	T_{max} (°C)	PI*	TOC**	HI†	OI†
930923-8	Parachute Creek Member mahogany shale	offshore open lacustrine	lat. 39°53′12″N long. 110°44′58″W	black marlstone	2.76	438	0.01	15.23	962	27
930923-6	upper black shale facies carbonate marker	offshore open lacustrine	lat. 39°51′28″N long. 110°45′54″W	dark-gray limestone	1.19	427	0.03	5.54	1031	44
930923-7	upper black shale facies carbonate marker	offshore/nearshore open lacustrine	lat. 39°51′26″N long. 110°45′54″W	dark-brown shale	1.12	429	0.02	6.58	940	46
930923-1	upper black shale facies long point bed	offshore/nearshore open lacustrine	lat. 39°51′28″N long. 110°45′54″W	dark-gray marlstone	0.48	442	0.02	3.38	981	28
930922-2	upper black shale facies long point bed	offshore/nearshore open lacustrine	lat. 39°51′28″N long. 110°45′54″W	medium-gray mudstone	0.46	434	0.04	1.78	749	48
TR1928	lower black shale facies	paludal	lat. 39°50′30″N long. 110°47′05″W	black coal	7.24	417	0.02	67.66	589	13
930922-1	lower black shale facies	nearshore open lacustrine	lat. 39°50′09″N long. 110°47′05″W	black/maroon marlstone	0.81	438	0.01	5.86	734	46

*$S_1/(S_1 + S_2)$.
**wt. % rock.
†mg HC/g TOC.

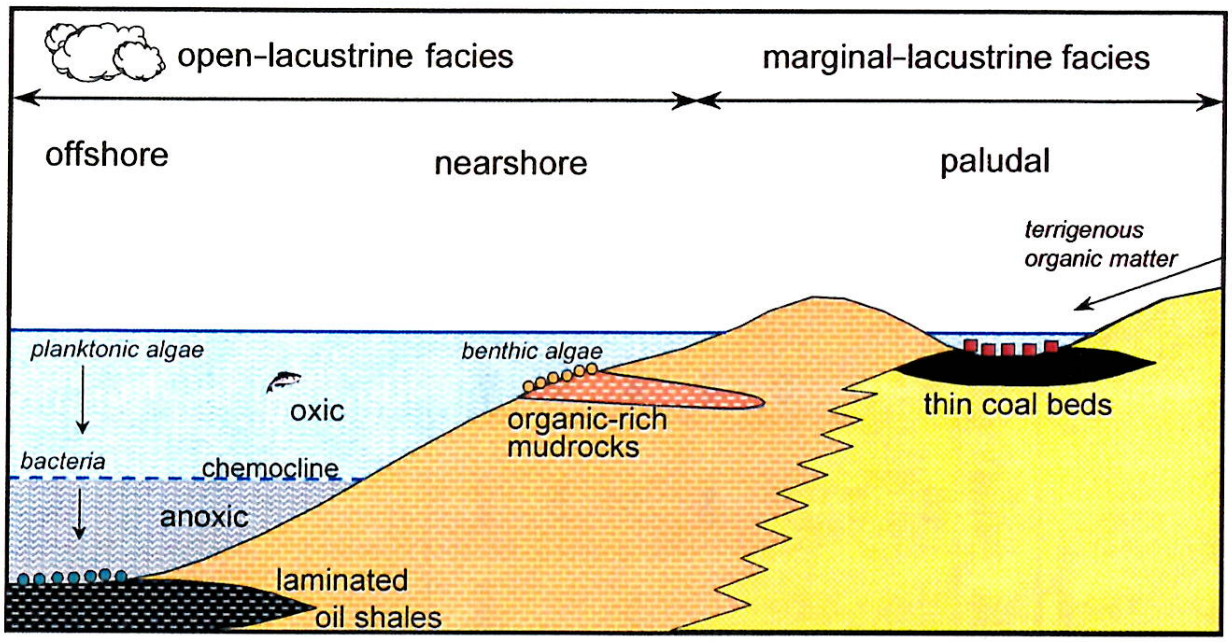

Figure 3. Schematic presentation of depositional settings in Lake Uinta responsible for source rock lithofacies of the Green River Formation. As discussed within the text, source rock types are defined by both the nature of their organic matter input and by their depositional setting.

of this biogenic-meromictic lake model are described in Desborough (1978).

Nearshore Open-Lacustrine Facies

The nearshore open-lacustrine facies is more proximal relative to the offshore depositional environment (Figure 3). The nearshore open-lacustrine facies (Fouch et al., 1976; Ryder et al., 1976; Wiggins and Harris, 1994) is equivalent to strata previously defined as lagoonal, shoal and transitional offshore (Williamson and Picard, 1974), shallow lacustrine (Lucas and Drexler, 1975), littoral- and sublittoral-lacustrine (Hanley, 1976), proximal open lacustrine (Cole and Picard, 1978), and nearshore lacustrine (Castle, 1990). A distinctive lithologic feature of this facies is the presence of organic-rich (type I kerogen), mollusk and ostracodal, mud-supported limestones. Unlike their deeper water equivalents, these low-grade oil shales are not distinctively laminated but contain very fine particulate organic matter along with streaked and rounded coal/charcoal(?) fragments dispersed in a thick- and medium-bedded limestone matrix (Ryder et al., 1976; Wiggins and Harris, 1994). Charophytes are abundant, suggesting that colonies of benthic cyanobacteria and algae were the probable sources for the preserved organic material (Robbins, 1987). The source rock is interpreted to have originated in quiet-water, shallow, lacustrine habitats, possibly lagoons formed along the margins of Lake Uinta.

Although the low-grade oil shales are diagnostic of the nearshore open-lacustrine facies, this subenvironment shows more lithologic diversity than the other lacustrine facies (Williamson and Picard, 1974). For example, open-lacustrine siliciclastic bars, which formed parallel with the shoreline during periods of high fluvial discharge, are an important component of this facies and represent potential reservoir rocks (Williamson and Picard, 1974; Castle, 1990; Wiggins and Harris, 1994). Algal stromatolites are sometimes present as thin stringers extending from the marginal into the open-lacustrine facies (Williamson and Picard, 1974; Cole and Picard, 1978). In addition to lithologic diversity, complex variations in the sedimentary structures and fossil assemblages also record numerous shoreline fluctuations or depositional cycles in this shallow-lacustrine environment (Hanley, 1976). Wiggins and Harris (1994) noted at least 20 short-term shallowing-upward cycles in the nearshore lacustrine deposits of the black shale facies (see Figure 2) at Soldier Summit, Utah. The complex lateral and vertical facies variations in the nearshore open-lacustrine en-

vironment preclude a simple lithologic description similar to the laminated oil shales in the offshore open-lacustrine facies.

Paludal Facies

Although Tertiary lacustrine coal deposits in the Uinta basin are small, their paleoecological and organic geochemical significance is very important. As such, the paludal facies is considered a discrete marginal lacustrine source rock unit in this investigation (Figure 3), following Fouch (1975), who chose to classify paludal sediments within his alluvial facies. Peat-forming depositional environments are thought to have formed in quiet, freshwater, vegetated settings at the fluctuating margin of Lake Uinta (Hanley et al., 1976; Franczyk et al., 1989). Because true grasses did not become abundant until the Miocene (Leopold, 1969), woody trees and shrubs dominated Lake Uinta wetlands, which would be specifically classified as swamps (Cowardin et al., 1979; Robbins, 1987). Palynological analyses of comparable lacustrine coals in the Vermillion Creek basin, Wyoming, suggests that they formed in a moist, subtropical climate where the local peat-forming flora were dominated by angiosperms (palms) and ferns (Nichols, 1987). The coal deposits in the Uinta basin have a limited thickness/lateral extent and are commonly interbedded with organic-rich carbonates (Ryder et al., 1976). These observations strongly suggest that the peat-forming swamps were not widespread but represent a restricted ecosystem within carbonate mudflats or ponds in the interdeltaic setting.

Tertiary lacustrine coals have been reported to be comparable to a high-grade oil shale, and samples from the Willow Creek Canyon yield as much as 79 gallons of oil per ton (Hanley et al., 1976). The maceral commonly associated with oil shales is alginite; consequently, these coals have previously been referred to as "algal coals" (Ryder et al., 1976). Petrographic analyses of the coals in the Uinta basin (Hutton, 1988; Wiggins and Harris, 1994; B. Cardott, 1994, personal communication) and the Vermillion Creek basin (Stanton et al., 1987), however, show that they are dominated by vitrinite (telocollinite), having minor liptinite (resinite/fluorinite, cutinite) and lacking inertinite and alginite. These results are consistent with the palynological evidence that shows that vascular plants, not algae, were the dominant precursors of the organic matter preserved in the lacustrine coals. This evidence distinguishes the open-lacustrine oil shales from the marginal lacustrine coals and serves to define another unique, albeit minor, source facies within the Green River petroleum system. For further information on the sedimentology and depositional history of the Uinta basin, see Porter (1963), Ryder et al. (1976), Boyer (1982), Johnson (1985), Picard (1985), Franczyk et al. (1989), and Ruble and Philp (1998).

LABORATORY SIMULATION OF PETROLEUM GENERATION

We used hydrous pyrolysis to assess the products and mechanisms of oil generation in samples from the Green River Formation. In this procedure, 250–500 g of crushed source rock chips ranging in size from 0.5 to 2 cm are heated isothermally in 1 L reaction vessels at temperatures between 160 and 365°C for 12 to 720 hr in the presence of liquid water (see Ruble [1996] and Ruble and Philp [1998] for details). The amounts of four main organic phases in the closed-system pyrolysis experiments (gases, oils, bitumens, and kerogen) vary systematically with thermal maturity. Changes in the compositions of organic phases occur because of complex physiochemical transformations during maturation. Although considerable data on the distribution and composition of organic phases from hydrous pyrolysis studies exist in the literature (e.g., Lewan, 1985; Eglinton et al., 1988; Peters et al., 1990; Michels and Landais, 1994), only limited data are available on hydrous pyrolysis of Green River shale (Huizinga et al., 1988). Defining the organic phases and documenting changes with maturity is important to establish the theoretical basis for calculating oil-generation kinetics, and it provides new insights to explain the natural occurrence of various hydrocarbon products in the Green River petroleum system.

Quantitative Yields

Quantitative generation curves (mg/g TOC) for four different organic phases were followed with increasing thermal maturity throughout the 72 hr temperature maturation series (Figure 4; Tables 2, 3). These four phases represent (1) total hydrocarbon gases, (2) immiscible oil floating on the water, (3) solvent extractable bitumen from the rock chips, and (4) insoluble residual kerogen. In general, yields of the different organic phases follow very similar trends for both Green River source facies (mahogany shale and black shale facies). These trends are characterized by an early stage of bitumen generation, which coincides with decreased

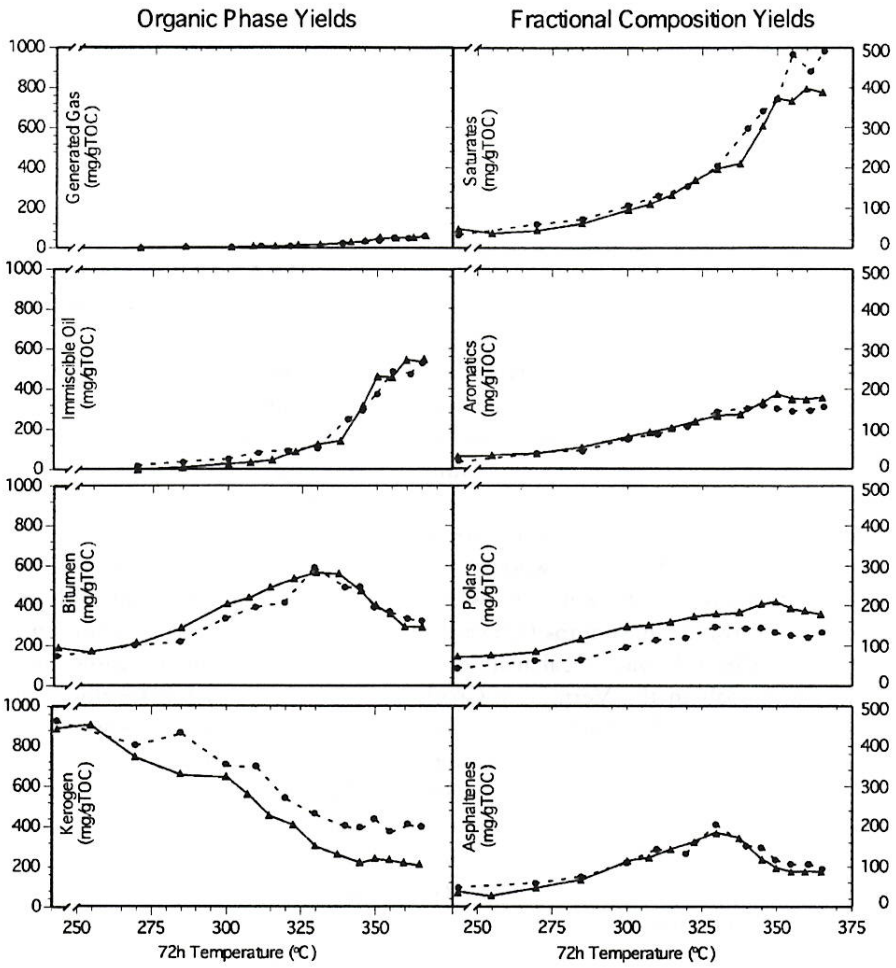

Figure 4. Evolution of organic phases and total fractional yields during artificial maturation. Quantitative yields of hydrocarbon gases, immiscible oil, bitumen, and kerogen from the 72 hr hydrous pyrolysis experiments are shown for both the mahogany shale (black triangle) and black shale facies (black circle) source rocks. Quantitative yields of saturates, aromatics, polars, and asphaltenes from the 72 hr hydrous pyrolysis experiments include combined yields from both the bitumen and immiscible oil phases. See Ruble (1996) for quantification methods.

kerogen in the source rocks (Figure 4). This low-maturity bitumen generation stage is followed by a main stage of immiscible oil generation. The bitumen generation stage maximizes at 330°C/72 hr and then shows a sharp decline as yields of immiscible oil rapidly increase (Figure 4). These observations are consistent with previously reported hydrous pyrolysis data from the Green River shale (Huizinga et al., 1988) and strongly support a product-precursor relationship between the immiscible oil and bitumen phases (Lewan, 1994). The hydrocarbon gases show a slight increase during the main stage of oil generation (Figure 4). The absence of significant thermal cracking, however, is demonstrated by the continued increase in immiscible oil yields at the highest maturity levels. Experimental conditions in this investigation were selected primarily to examine oil and associated gas generation, thus, high-maturity thermal cracking processes were negligible under the chosen conditions. Although the mahogany shale had much higher initial total organic carbon (TOC) content than the black shale facies (15.23 vs. 5.86%), the overall total product yields of gas, oil, and bitumen for both source facies pyrolysates were virtually identical when normalized to mg/g TOC (Figure 4), suggesting similar hydrocarbon generative potential and similar kinetics for each of these type I kerogens.

Fractional Compositions

Laboratory simulation experiments are conducted in a closed system, which allows calculations of the quantitative distributions of various organic fractions with increasing thermal maturity. In this investigation, the cumulative yields (bitumen + immiscible oil) of four fractions (saturates, aromatics, polars, and asphaltenes) were determined from fractional composition data and quantitative organic phase measurements (Figure 4; Tables 2, 3). Asphaltenes were separated from the

Table 2. Quantitative Yields and Fractional Compositions of Various Organic Phases from the Mahogany Shale (930923-8) 72 Hr Hydrous Pyrolysis Experiments*

	Temp (°C)/Time (Hr)																			
	Unheated	160/72	180/72	200/72	220/72	240/72	255/72	270/72	285/72	300/72	307.5/72	315/72	322.5/72	330/72	337.5/72	345/72	350/72	355/72	360/72	365/72
mg Kerogen/g TOC	884.4	1066.3	982.3	910.7	848.9	964.5	904.1	744.6	658.6	647.4	560.7	455.7	410.4	304.0	262.6	223.2	242.3	235.1	221.3	210.1
mg Bitumen/g TOC	181.0	132.3	123.0	146.0	149.6	148.6	163.0	204.0	280.8	401.4	432.3	483.0	526.1	557.9	550.7	465.7	393.5	353.2	290.0	288.4
mg Oil/g TOC	0	0	0	0	0	0	0	0	9.2	28.1	35.4	46.5	88.6	125.8	142.8	318.4	465.7	461.5	549.3	537.5
mg Gas/g TOC	0	0	0	0	0	0	0	2.1	2.7	5.1	7.5	9.5	14.0	17.9	22.1	32.8	47.5	50.3	51.2	57.2
mg Sat/g TOC	46.4	37.3	32.8	37.4	35.7	35.3	35.0	42.0	59.3	93.9	108.7	131.9	168.5	197.1	209.7	302.5	371.7	365.1	396.7	386.9
mg Arom/g TOC	32.0	29.4	27.7	32.9	31.3	31.6	33.3	38.0	53.8	80.3	92.0	102.5	119.2	133.3	136.6	166.7	187.6	175.6	174.4	178.8
mg Polar/g TOC	68.0	51.7	50.3	60.9	61.3	63.3	69.7	79.6	111.5	142.7	146.8	154.5	167.7	174.1	178.2	198.7	204.9	188.1	182.4	174.5
mg Asph/g TOC	34.6	13.9	12.2	14.7	21.3	18.4	24.9	44.5	65.4	112.6	120.2	140.6	159.3	181.2	169.0	116.2	95.1	85.7	85.9	85.7
Bitumen %sat	25.7	28.2	26.7	25.6	23.9	23.8	21.5	20.6	18.7	18.4	19.5	20.6	20.3	20.7	21.5	24.2	26.4	26.9	27.9	28.7
Bitumen %arom	17.7	22.2	22.5	22.5	20.9	21.3	20.4	18.6	18.8	19.1	20.2	19.9	20.4	20.5	20.7	23.6	25.1	24.5	23.0	23.3
Bitumen %polar	37.6	39.1	40.9	41.7	41.0	42.6	42.8	39.0	39.2	34.6	32.8	30.7	29.6	27.8	28.1	29.5	28.6	29.0	26.9	25.0
Bitumen %asph	19.1	10.5	9.9	10.1	14.2	12.4	15.3	21.8	23.2	27.8	27.5	28.8	29.7	31.1	29.7	22.6	19.9	19.5	22.2	23.0
Oil %sat	No oil	No oil	No oil	No oil	No oil	No oil	No oil	No oil	72.6	70.7	68.5	69.7	69.8	63.9	63.9	59.5	57.5	58.5	57.5	56.6
Oil %arom									10.1	12.2	13.7	13.6	13.4	15	15.6	17.8	19.1	19.3	19.6	20.7
Oil %polar									14.8	14.0	14.4	13.2	13.6	15	16.4	19.3	19.8	18.6	19.0	19.0
Oil %asph									2.5	3.1	3.4	3.4	3.2	6.1	4.0	3.4	3.6	3.6	3.9	3.6

*Yields are reported as mg/g $TOC_{original}$.

Table 3. Quantitative Yields and Fractional Compositions of Various Organic Phases from the Black Shale Facies (930922-1) 72 Hr Hydrous Pyrolysis Experiments*

	Temp (°C)/Time (Hr)												
	Unheated	270/72	285/72	300/72	310/72	320/72	330/72	340/72	345/72	350/72	355/72	360/72	365/72
mg Kerogen/g TOC	919.8	807.2	865.2	704.8	696.2	540.9	462.5	402.7	394.2	436.9	375.4	411.3	399.3
mg Bitumen/g TOC	138.6	195.1	211.6	328.3	385.0	408.6	582.1	485.2	487.1	385.8	364.3	327.9	318.4
mg Oil/g TOC	0	17.7	37.3	50.7	84.8	96.8	112.1	252.2	299.6	381.3	490.3	480.4	551.6
mg Gas/g TOC	0	n.d.	4.1	2.4	8.5	7.3	15.8	26.9	30.3	35.8	44.1	50.4	58.7
mg Sat/g TOC	33.8	58.9	70.9	104.9	130.9	153.3	204.4	298.1	341.0	370.7	483.4	439.9	491.6
mg Arom/g TOC	20.8	39.6	45.9	74.7	88.2	107.2	144.5	152.1	160.5	152.3	145.8	147.7	156.9
mg Polar/g TOC	38.7	58.3	59.9	91.4	109.5	115.1	142.7	138.2	140.1	129.2	121.5	116.6	129.3
mg Asph/g TOC	45.2	56.0	72.2	108.0	141.1	129.8	202.7	149.0	145.1	114.9	104.0	104.2	92.2
Bitumen %sat	24.4	23.5	20.1	20.4	18.0	21.6	22.2	26.8	27.4	29.9	34.6	36.1	34.2
Bitumen %arom	15.0	19.6	20.3	21.3	20.2	23.4	22.6	24.1	24.8	25.2	24.2	23.2	22.1
Bitumen %polar	28.0	29.2	27.0	26.4	26.4	25.2	22.1	21.7	20.9	21.0	20.3	19.4	22.0
Bitumen %asph	32.6	27.7	32.6	31.9	35.4	29.8	33.1	27.4	26.9	24.0	20.9	21.3	21.7
Oil %sat	No oil	74.4	76.1	74.9	72.8	67.1	66.8	66.6	69.2	66.9	72.9	66.9	69.4
Oil %arom		7.1	8.1	9.6	12.2	11.9	11.6	13.9	13.2	14.5	11.8	14.9	15.7
Oil %polar		7.9	7.3	9.1	9.1	12.5	12.4	13.1	12.8	12.7	9.7	11.0	10.7
Oil %asph		10.5	8.5	6.4	5.9	8.5	9.2	6.3	4.7	5.9	5.7	7.1	4.2

*Yields are reported as $mg/gTOC_{original}$.

maltene fraction of the samples by precipitation with n-pentane (Ruble, 1996). The maltene fraction was separated by liquid chromatography using 5 mL alumina/silica columns eluted successively with n-pentane, benzene, and 60:40 wt. % benzene/methanol, enabling the isolation of the saturate, aromatic, and polar fractions, respectively (Ruble, 1996).

A direct product-precursor relationship between the immiscible oil generated during hydrous pyrolysis and the bitumen component formed during thermal breakdown of the kerogen has been previously suggested (Lewan, 1991, 1994). Lewan (1997) described the processes thought to occur during hydrocarbon generation in the hydrous pyrolysis system. These processes happen in three stages: (1) bitumen generation, (2) immiscible oil generation, and (3) pyrobitumen/gas generation. Kerogen decomposition to bitumen involves cleavage of weak noncovalent bonds at low maturity, producing a substance enriched in high molecular-weight hydrocarbons and heteroatom components (Lewan, 1993). At higher maturity, the bitumen that is saturated with dissolved water undergoes partial decomposition, producing aliphatic moieties that form an immiscible oil phase (Lewan, 1994). This immiscible oil phase is expelled from the source rock during primary migration and is collected from the surface of the water at the completion of each hydrous pyrolysis experiment. At higher maturity, the expelled oil and retained bitumen eventually decomposes into gas and pyrobitumen (Lewan, 1993).

Our quantitative compositional data show these three stages of generation. In the primary stage of bitumen generation (<330°C/72 hr), the quantities of all fractions increase with increasing pyrolysis temperature (Figure 4). The saturates and asphaltenes, however, appear to increase faster than the polars and aromatics (Figure 4), presumably due to the highly aliphatic nature of these type I kerogens. At the peak of bitumen generation (330°C/72 hr) the asphaltenes show a sharp decrease, whereas the saturates show an even greater parallel increase in concentration (Figure 4). These results suggest that the conversion of bitumen to immiscible oil could be described as conversion of asphaltenes to saturated hydrocarbons. Such a process is consistent with the free radical mechanism of immiscible oil generation outlined by Lewan (1994) and hydrous pyrolysis experiments on asphaltenes (Jones et al., 1988). Our data further support this interpretation because as the rate of asphaltene degradation slows at high-maturity levels, indicating that the asphaltenes have exhausted their generative capacity, the rate of saturates/immiscible oil generation also

slows (Figure 4). In contrast to this clear product-precursor relationship, the polar and aromatic generation curves appear to increase relatively uniformly with maturity to peak oil generation and are independent of the saturate and asphaltene curves. This observation suggests that the polars and aromatics originate mainly from the kerogen and that, although they may become more concentrated in the immiscible oils at higher maturity, they are not driving the process of immiscible oil generation. Some of the complexities in the generation curves of the polar and aromatic fractions at high maturity levels are probably due to the competing processes of generation/degradation.

A different method for distinguishing variations in fractional composition is via the use of ternary diagrams. Lewan (1997) used a ternary plot of saturates, aromatics, and polars + asphaltenes to illustrate the differences in composition between expelled immiscible oils vs. retained bitumens and to compare experimentally derived data to a suite of natural oils and bitumens. Data from our investigation are consistent with previous trends (Peters et al., 1990; Lewan, 1991) and clearly distinguish the immiscible oils, which are enriched in saturates, from the extracted bitumens, which are enriched in polars and asphaltenes (Figure 5). Maturation trends in the bitumens show a general increase in the

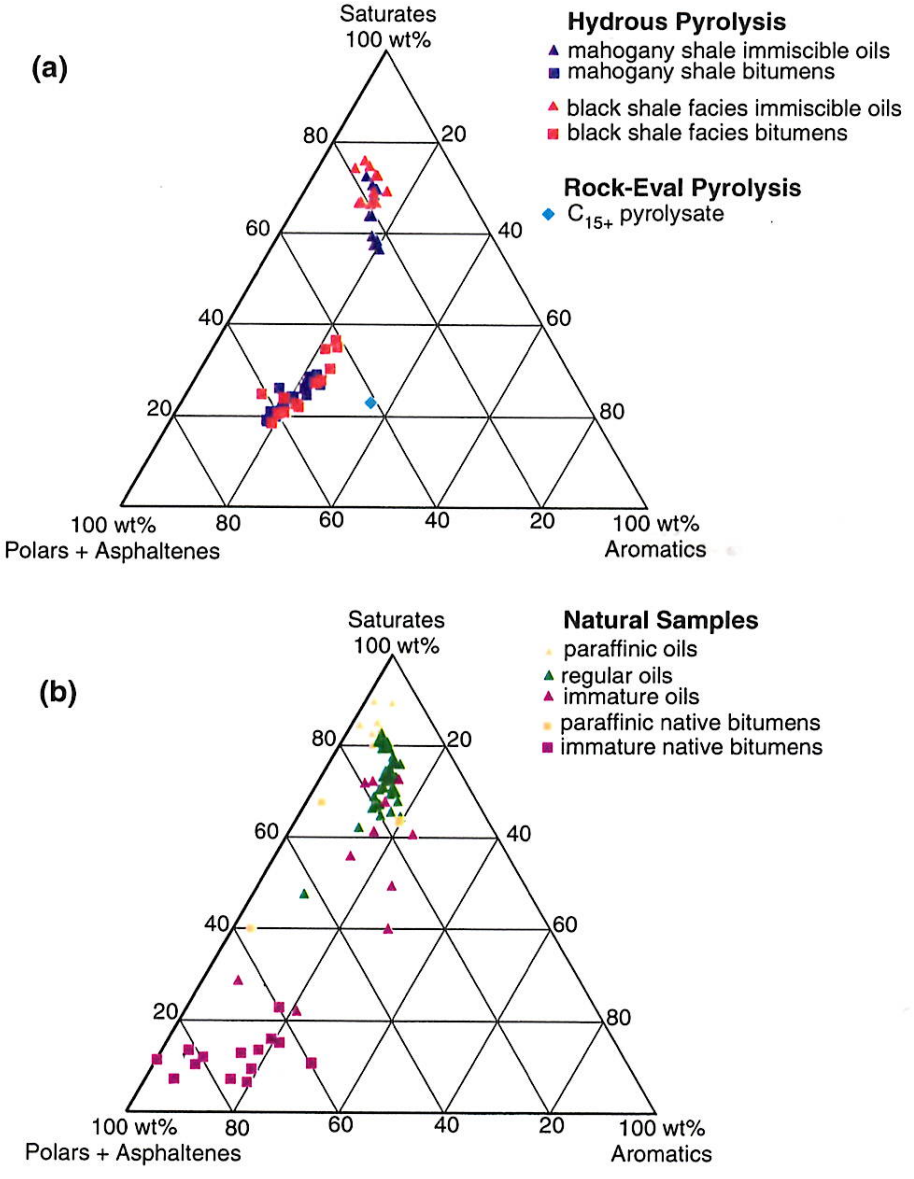

Figure 5. Ternary diagrams comparing the fractional composition of the products from (a) artificial maturation pyrolysis experiments and (b) a suite of natural samples from the Uinta basin. For the hydrous pyrolysates, note the clear compositional distinction between expelled immiscible oils and the retained bitumen phase. In contrast, data from Behar et al. (1997) show that the composition of open-system pyrolysates more closely resembles bitumen. Uinta basin crude oil data and classifications adapted from Mueller (1998).

proportion of saturates during immiscible oil generation as asphaltenes are converted into aliphatic hydrocarbons. In contrast, the immiscible oils are characterized by a decrease in the relative proportion of saturates with increased thermal maturity as aromatic and polar concentrations increase in the expelled oils.

Experimentally derived pyrolysis products have also been compared to a representative suite of naturally occurring hydrocarbons from the Uinta basin, which include crude oils and various types of semisolid and solid native bitumens (Figure 5). Paraffinic crude oils associated with deep, overpressured reservoirs (group I in Fouch et al. [1994]) in the Altamont field show somewhat higher proportions of saturates compared to the waxy immiscible oils generated during pyrolysis of the Green River source rocks (Figure 5). This is consistent with other suites of samples where the oils and bitumens generated by hydrous pyrolysis have slightly higher aromatic/polar content than natural crude oils and bitumens (Lewan, 1997). In contrast, low-maturity aromatic-intermediate and aromatic-asphaltic oils associated with shallow reservoir rocks (group II in Fouch et al. [1994]) are depleted in saturates compared to the immiscible oils generated by hydrous pyrolysis (Figure 5). Two of these natural samples are semisolid gilsonite tars, and one is a shallow drill-stem test (DST) oil from the Altamont field. The fractional compositions of these samples more closely correspond to hydrous pyrolysis bitumens than to immiscible oils, and one sample plots within the zone of experimental bitumens (Figure 5). We suggest that these samples are not true oils because they do not represent a natural phase separation between bitumen and oil. Instead, samples such as these are thought to represent expelled bitumens, which arise as a consequence of bitumen generation in extremely organic-rich source rocks where bitumen formation exceeds the capacity of the rock to retain this organic phase prior to immiscible oil formation. Such a process may explain early hydrocarbon expulsion, previously reported in some organic-rich lacustrine sequences (Qiang et al., 1997; Katz and Xingcai, 1998; Qiang and McCabe, 1998).

Early bitumen generation may also be responsible for some of the unusual native bitumen deposits in the Uinta basin (Hunt, 1963; Ruble, 1990). Aromatic-asphaltic bitumens, such as gilsonite, show greater proportions of polar constituents compared to hydrous pyrolysis bitumens (Figure 5). This is most likely a consequence of secondary alteration effects associated with devolatilization and possibly limited biodegradation of these native bitumens. Samples of the paraffinic bitumen ozocerite do not correlate well with the hydrous pyrolysis bitumens but are similar in composition to the immiscible oils (Figure 5). These samples likely originate as expelled paraffinic oils that were subsequently altered by devolatilization, reducing the proportion of low molecular weight compounds and enhancing the abundance of the extremely high molecular weight (>n-C_{50}) waxes (Ruble, 1990; Philp et al., 1995).

PETROLEUM CHARACTERIZATION AND CORRELATION

Crude Oil Characterization

The immiscible oils generated during hydrous pyrolysis were compared with four DST oils from various stratigraphic intervals in the Texaco D-1 Ute Tribal well from the Altamont field in the northeastern Uinta basin (Figure 1). We consider these four DST oils to be representative of most of the types of crude oils in the Uinta basin. Stratigraphic associations for these oils (Table 4) and the general depth relationships in a nearby core (Picard et al., 1973) show that the shallowest oil (4700 ft [1433 m]) is associated with reservoirs in the upper part of the Green River Formation (group II in Fouch et al. [1994]), whereas the deeper oils (>8500 ft [2591 m]) are from overpressured reservoirs in the basal Green River/Wasatch (group I in Fouch et al. [1994]). The shallowest sample is viscous, black, and heavy, whereas the deeper samples are waxy solids at room temperature and have colors ranging from black to yellow with increasing depth. Others noted similar differences with depth for paraffinic crude oils from the Altamont-Bluebell trend (Lucas and Drexler, 1975; Montgomery and Morgan, 1998). Oil from Green River reservoirs (carbonate marker equivalent) is typically a black wax that contains greater than 12% paraffins and has a pour point of up to 120°F (46°C) and a gravity of 33° API (Montgomery and Morgan, 1998). Crude from the underlying Flagstaff–Colton reservoirs (lower black shale facies equivalent) is a yellow wax that consists of 7–8% paraffins, a pour point near 90–95°F (30–33°C), and a gravity of 39° API (Montgomery and Morgan, 1998).

Whole-oil gas chromatograms and fractional data for the four samples (Figure 6) show compositional differences between the shallow and deeper Uinta basin crude oils. The 4700 ft [1433 m] DST oil contains a

Table 4. Sample Identifications, Locations, and Molecular Maturity Ratios in the Texaco D-1 Ute Tribal DST Oils*

Sample Number	Stratigraphic Unit	Depth	Location	Sample Characteristics	CPI 1**	Pristane/n-C_{17}	Phytane/n-C_{18}	C_{29} ααα Steranes 20S/(20S + 20R)	C_{29} Steranes αββ/(αββ + ααα)
90103-21	saline facies†	4700 ft (1433 m)	lat. 40°13′18″N long. 110°31′40″W	black heavy oil	1.65	2.29	4.25	0.34	0.29
90103-18	upper black shale facies	8569–8632 ft (2612–2631 m)	lat. 40°13′18″N long. 110°31′40″W	black wax	1.00	0.41	0.35	0.34	n.d.
90103-19	lower black shale facies	9251 ft (2820 m)	lat. 40°13′18″N long. 110°31′40″W	brown wax	1.01	0.20	0.10	n.d.	n.d.
90103-20	lower black shale facies	10217–10317 ft (3114–3145 m)	lat. 40°13′18″N long. 110°31′40″W	yellow wax	1.02	0.17	0.08	n.d.	n.d.

*n.d. = No data.
**Hunt (1979).
†340 ft (104 m) above mahogany bed.

high proportion of aromatic and resin components (~50%) and would be classified as an aromatic-intermediate crude oil (Tissot and Welte, 1978). The gas chromatogram of this shallow oil is dominated by β-carotane and other acyclic isoprenoids. This sample also contains relatively high abundances of terpanes and steranes, which are present in approximately equal proportion to the n-alkanes. In contrast, chromatograms for the deeper (>8500 ft [2591 m]) DST oils are dominated by n-alkanes (Figure 6). Compared to the shallow sample, these oils show more n-alkanes relative to isoalkanes and a higher proportion of long-chain components (>C_{20}), with some alkanes extending past C_{50}. The waxy oil at 8569 ft [2612 m] shows a distinct bimodal distribution of n-alkanes that have maxima at C_{15} and C_{28}; however, deeper samples do not exhibit this feature (Figure 6). Also a clear trend exists of increasing proportion of saturates in these paraffinic oils with increasing depth.

A variety of molecular ratios and quantitative data have been calculated from gas chromatography (GC) and gas chromatography–mass spectrometry (GCMS) analyses of the crude oils (Table 4). The carbon preference index (CPI) and odd-even predominance (OEP) ratios indicate a distinct odd predominance in the n-alkanes (CPI 1.65) for the 4700 ft [1433 m] sample. The deeper paraffinic DST oils, however, show uniform distributions in their alkanes and no carbon number predominance. Isoprenoid/alkane ratios are high (>1) in the 4700 ft [1433 m] sample but are lower in the three waxy oils (<1) and decrease with depth in these deeper samples. Pristane/phytane (Pr/Ph) ratios are variable, but all samples have values greater than 1. Sterane biomarker ratios have been determined for the 4700 ft [1433 m] sample, but concentrations were generally insufficient to permit their determination in the deeper paraffinic DST oils (Table 4). Sterane maturity ratios in the 4700 ft [1433 m] sample are generally below proposed thermal endpoint values, suggesting that this sample is in the low-maturity stage of oil generation (Peters and Moldowan, 1993). Although not definitive, the single sterane maturity parameter available for the DST oil at 8569 ft [2612 m] also suggests a low to early mature generation stage (Table 4).

Crude Oil–Immiscible Oil Correlation

Maturation Series–Mahogany Shale and Black Shale Facies

To determine closed-system kinetic parameters, a suite of time-temperature hydrous pyrolysis experiments

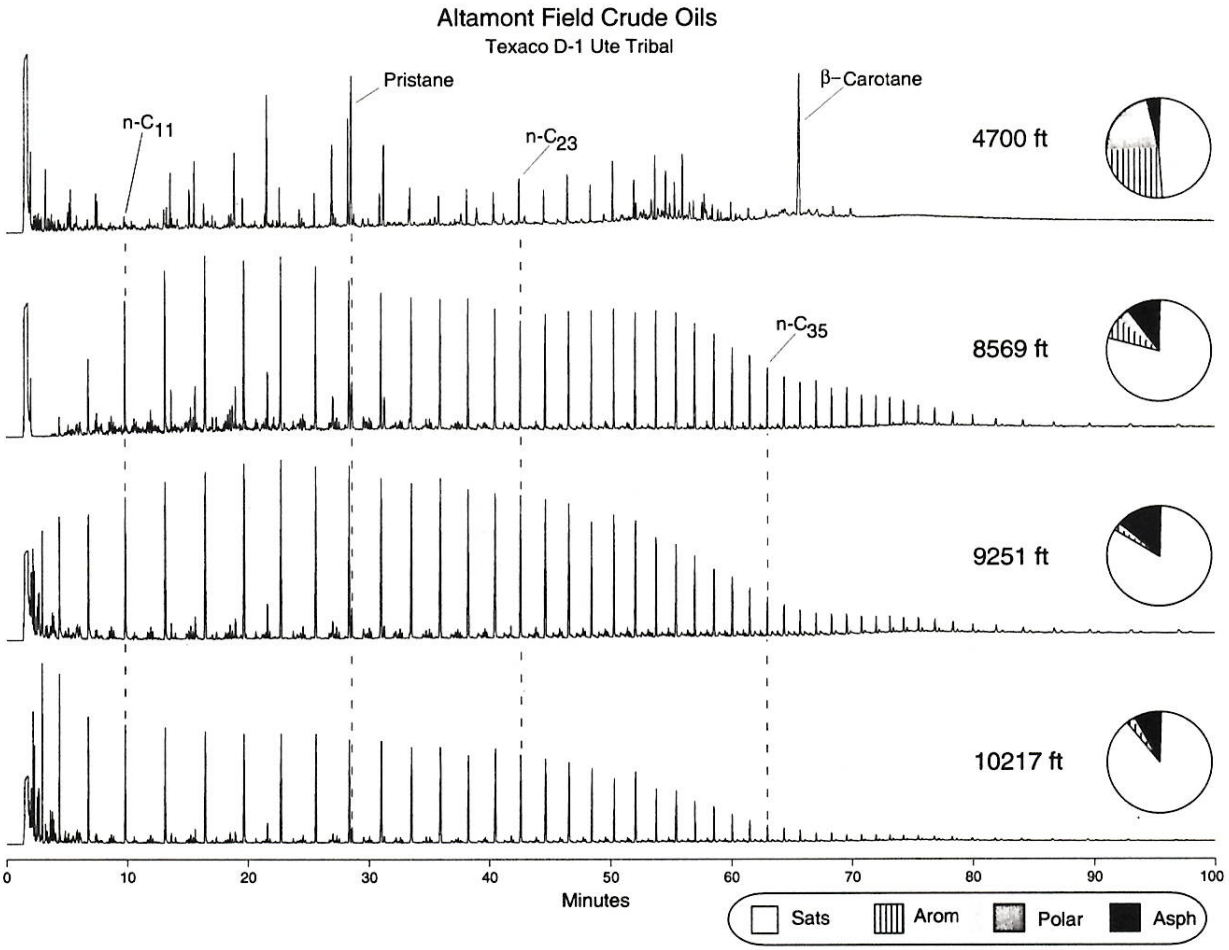

Figure 6. Whole-oil gas chromatograms and fractional compositions for selected DST oils from the Texaco D-1 Ute Tribal well, Altamont field, Uinta basin. These samples are representative of the different types of crude oils in the Uinta basin. Conditions of analysis are described by Ruble (1996), and further sample details are given in Table 4.

were performed on two distinct Green River Formation source facies, referred to informally as the mahogany shale and the black shale facies (Figure 2). These experiments provide geochemical information for correlation of the expelled immiscible oils generated during hydrous pyrolysis with the various types of naturally occurring Uinta basin crude oils. These data can be used to examine the oil–source rock relationships and to assess the maturity of the natural crude oils relative to the simulated maturation series.

Physical characteristics are useful to correlate the natural crude oils with the experimentally derived immiscible oils. The immiscible oils from the mahogany shale varied from black, viscous, heavy oils at low maturities to more free-flowing, black oils at higher maturity. The low-maturity mahogany shale immiscible oils show physical characteristics similar to the shallow 4700 ft [1433 m] DST oil from the Altamont field. In contrast, the immiscible oils generated during pyrolysis of the black shale facies were reddish brown, waxy solids at room temperature. Although there are color variations among the natural samples that could not be reproduced experimentally, the physical characteristics of the black shale facies waxy immiscible oils are similar in most respects to those of deeper (>8400 ft [2560 m]) DST oils from the Altamont field.

In addition to physical similarities, the molecular composition of the immiscible oils determined by GC are also similar to the natural oils. Selected chromatograms illustrating maturation trends in the immiscible oils from the two Green River source facies are shown

in Figures 7 and 8, whereas the complete set of chromatograms is documented elsewhere (Ruble, 1996). For the mahogany shale, the low-maturity immiscible oils are dominated by acyclic isoprenoids that have lesser amounts of β-carotane, terpanes, steranes, and n-alkanes containing a strong odd predominance (Figure 7). This distribution of components is similar in most respects to the 4700 ft [1433 m] DST oil (Figure 6), although the relative abundance of biomarkers and β-carotane is lower in the immiscible oils generated during hydrous pyrolysis. Extractable bitumens from low-temperature mahogany shale hydrous pyrolysis, however, contain much higher abundances of biomarkers and β-carotane compared to the immiscible oils (Ruble, 1995, unpublished data). This observation further suggests that the sample from 4700 ft [1433 m] should be considered bitumen rather than true oil.

At elevated maturity, n-alkanes and aromatics become increasingly predominant in the mahogany shale immiscible oils, although the isoprenoids remain significant (Figure 7). The characteristic odd predominance in the n-alkanes is present in all of the mahogany shale immiscible oils. Although CPI values become lower with increasing simulated maturation (Table 5), an odd predominance is retained even at the highest maturity. For oil correlation purposes, there are no documented examples from the Uinta basin of natural analogs to the immiscible oils generated by high-maturity hydrous pyrolysis of the mahogany shale. Recent analyses of a comprehensive suite of crude oils from this petroleum system, however, indicate that more mature oils having some of these characteristics (e.g., odd predominance of n-alkanes) occur in reservoirs of the upper Green River Formation in the Altamont field (Mueller, 1998).

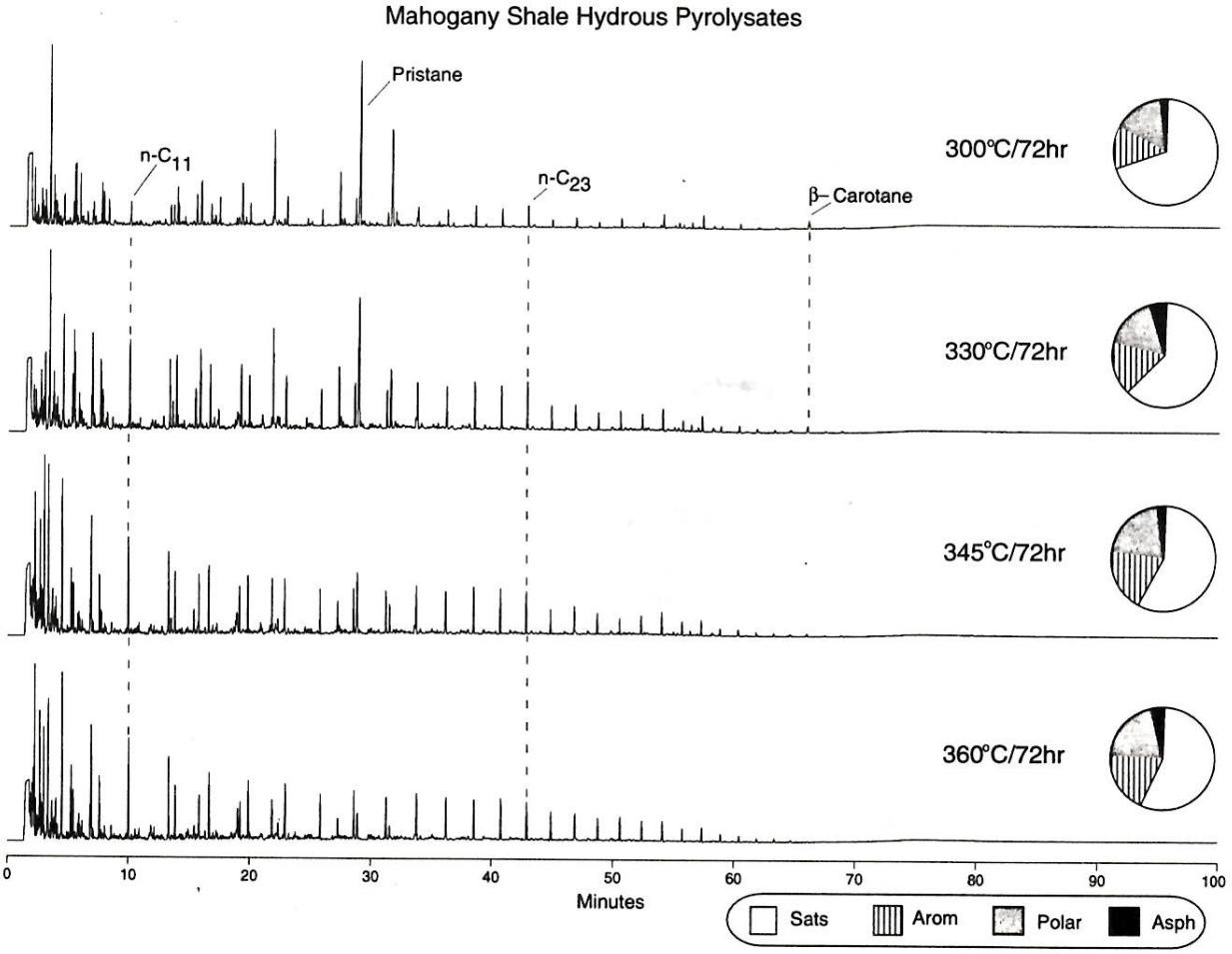

Figure 7. Whole-oil gas chromatograms and fractional compositions for selected immiscible oils generated during hydrous pyrolysis of the mahogany shale. Conditions of analysis are described by Ruble (1996).

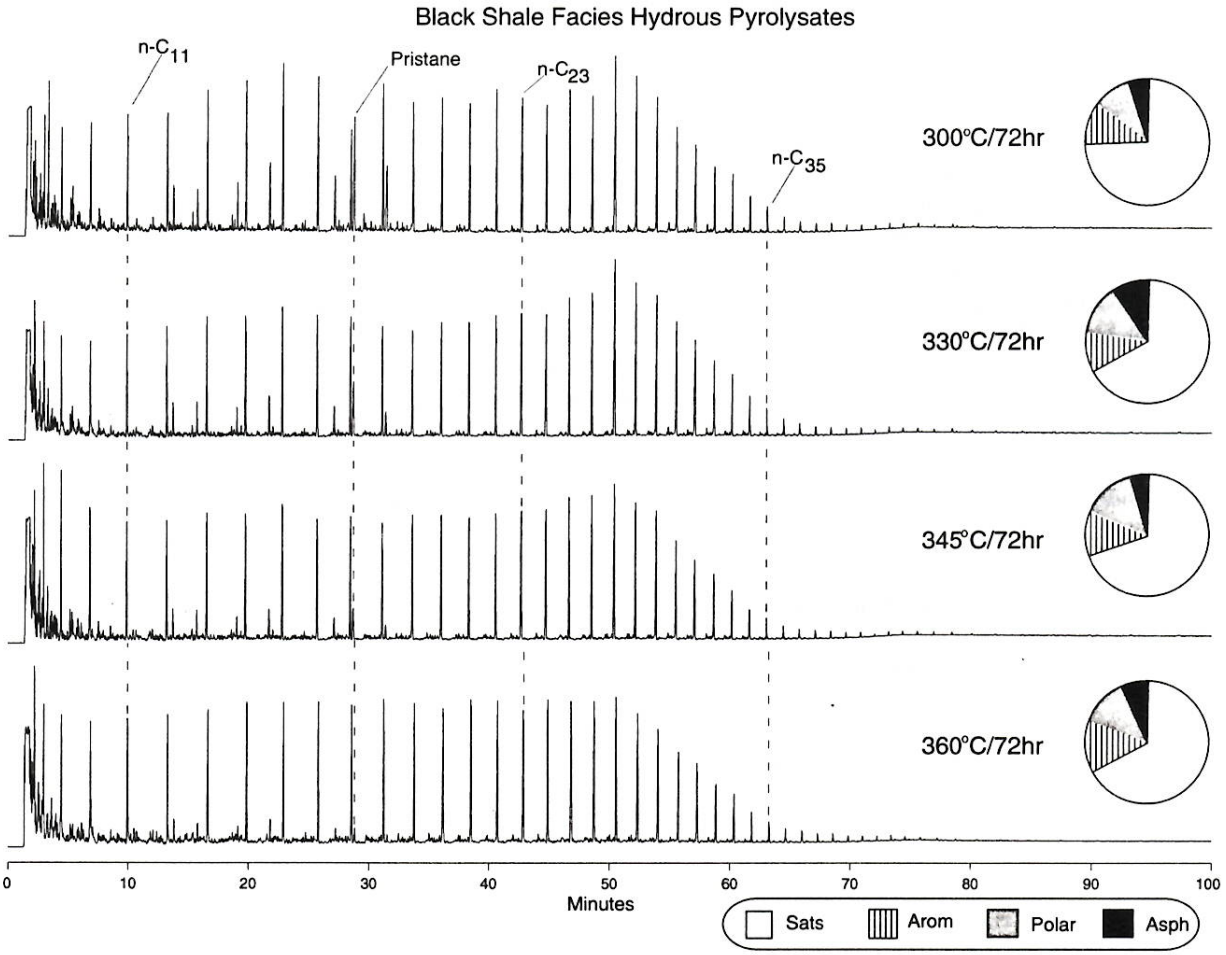

Figure 8. Whole-oil gas chromatograms and fractional compositions for selected immiscible oils generated during hydrous pyrolysis of the black shale facies. Conditions of analysis are described by Ruble (1996).

Table 5. Molecular Maturity Ratios in the Immiscible Oils from the Mahogany Shale (930923-8) 72 Hr Hydrous Pyrolysis Experiments*

	Temp (°C)/Time (Hr)										
Maturity Ratio	300/72	307.5/72	315/72	322.5/72	330/72	337.5/72	345/72	350/72	355/72	360/72	365/72
CPI 1**	2.16	2.06	1.98	1.59	1.54	1.52	1.34	1.28	1.24	1.21	1.18
Pristane/n-C_{17}	9.08	8.55	6.98	5.16	4.19	3.01	1.82	1.28	1.05	0.78	0.56
Phytane/n-C_{18}	9.43	7.10	4.43	2.82	2.12	1.63	0.96	0.71	0.54	0.43	0.32
C_{29} ααα steranes 20*S*/(20*S* + 20*R*)	0.15	0.14	0.19	0.22	0.26	0.24	0.33	0.57	n.d.	n.d.	n.d.
C_{29} steranes αββ/(αββ + ααα)	0.16	0.18	0.17	0.21	0.26	0.23	0.35	0.54	n.d.	n.d.	n.d.

*n.d. = No data.
**Hunt (1979).

The immiscible oils generated by hydrous pyrolysis of the black shale facies are solid waxes dominated by n-alkanes at all levels of maturity (Figure 8). Although these oils contain larger proportions of aromatics compared to the deeper Altamont crude oils, they are otherwise comparable. The low-maturity immiscible oils have isoprenoid/alkane ratios <1 (Table 6) and a bimodal distribution of n-alkanes that have maxima at C_{15} and C_{27}. These features are similar to those of the 8569 ft [2612 m] Altamont DST oil. With increasing simulated maturation, isoprenoid/alkane ratios decrease, and the bimodal distribution of alkanes shifts to lower molecular weight in the black shale facies immiscible oils, similar to the depth trend for the suite of paraffinic DST oils (Figure 6). For correlation purposes, three distinctive features link the deep paraffinic Uinta basin crude oils with immiscible oils from the black shale facies: (1) high molecular weight n-alkanes $>C_{40}$; (2) no carbon-number predominance in the n-alkanes at any level of maturity; (3) little to no β-carotane. These characteristics are obtained using conventional GC analyses and readily distinguish black shale facies oils from others in the Uinta basin.

More precise estimates of the thermal maturity of the natural crude oils compared to the suite of immiscible oils has been undertaken using a variety of molecular maturity parameters (Figure 9; Tables 4, 5, 6). Five maturity ratios for the 4700 ft [1433 m] Altamont DST oil were correlated with ratios from the immiscible oils generated by mahogany shale hydrous pyrolysis (72 hr temperature series) as follows: CPI (~330°C); Pr/n-C_{17} (337.5°C); Ph/n-C_{18} (322.5°C); αββ/(αββ + ααα) steranes C_{29} (~337.5°C); 20*S*/(20*S* + 20*R*) steranes C_{29}-ααα (345°C). The general maturation level of these ratios (~330°C/72 hr) corresponds to maximum bitumen generation from the mahogany shale (Figure 4) and is consistent with the interpretation that this oil sample represents an expelled bitumen associated with low-maturity thermal degradation of the kerogen in these organic-rich lacustrine source rocks. For the deeper paraffinic Altamont oils, less thermal maturity information is available for correlation with the black shale facies immiscible oils because CPI values in the immiscible oils showed no maturity variations and biomarker data were generally absent. Based primarily on isoprenoid/alkane ratios, however, the following maturation levels were determined for the three paraffinic Altamont DST oils: 8569 ft [2612 m] (~330°C); 9251 ft [2820 m] (350°C); and 10,217 ft [3114 m] (~360°C). This region (330–360°C/72 hr) brackets the main stage of immiscible oil generation from this source rock (Figure 4), which suggests that black shale facies type source rocks are present and generated paraffinic oil at various levels of maturity in the deeper parts of the Altamont field.

Additional Black Shale Facies Units

Based on Rock-Eval data (Table 1), one black shale facies source rock was selected for detailed investigation using a complete set of time-temperature hydrous pyrolysis experiments (sample 930922-1; lower black shale facies). Several other black shale facies source rock units, however, were also analyzed in a more limited manner. These samples include a coal (lower black shale facies) and four organic-rich limestones from the upper black shale facies (Figure 2; Table 1), including the carbonate marker and long point bed (Ruble and

Table 6. Molecular Maturity Parameters in the Immiscible Oils from the Black Shale Facies (930922-1) 72 Hr Hydrous Pyrolysis Experiments*

	Temp (°C)/Time (Hr)									
Maturity Ratio	300/72	310/72	320/72	330/72	340/72	345/72	350/72	355/72	360/72	365/72
CPI 1**	1.09	1.08	1.07	1.06	1.05	1.05	1.05	1.05	1.04	1.04
Pristane/n-C_{17}	0.96	0.93	0.79	0.63	0.39	0.36	0.23	0.18	0.15	0.09
Phytane/n-C_{18}	0.60	0.48	0.38	0.30	0.18	0.16	0.11	0.09	0.08	0.06
C_{29} ααα steranes 20*S*/(20*S* + 20*R*)	0.22	0.31	0.34	0.42	0.51	0.37	0.38	n.d.	n.d.	n.d.
C_{29} steranes αββ/(αββ + ααα)	0.24	0.26	0.32	0.39	0.53	0.47	n.d.	n.d.	n.d.	n.d.

*n.d. = No data.
**Hunt (1979)

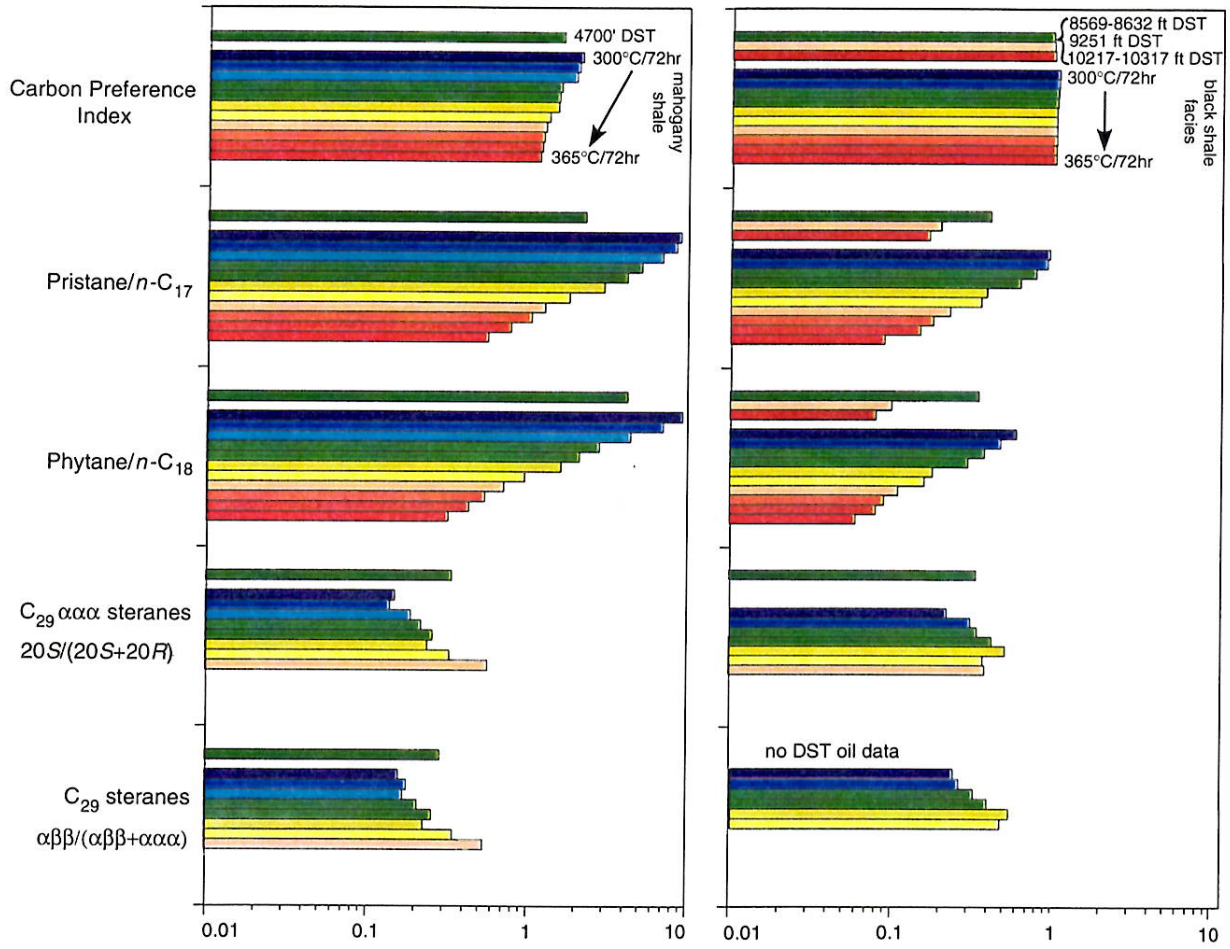

Figure 9. Selected molecular maturity ratios for DST oils and immiscible oils generated during hydrous pyrolysis of both the mahogany shale and black shale facies samples (log scale). Correlation of the 4700 ft (1433 m) DST oil with pyrolysates from the mahogany shale and the remaining DST oils with pyrolysates from the black shale facies is based on similar compositions (see text). Values for the ratios are in Tables 4–6.

Philp, 1998). To examine the character of oil generated from these units, a single hydrous pyrolysis experiment near the middle zone of immiscible oil generation (345°C/72 hr) was conducted using each of the different source rocks. The immiscible oils from these additional experiments were compared to the suite of DST oils and to immiscible oils of equivalent maturity from the previous experiments on the mahogany shale and black shale facies source rocks.

Gas chromatograms of the immiscible oils generated during hydrous pyrolysis (345°C/72 hr) of the various Green River source facies (Figure 10) illustrate the diversity of potential source rocks in the Uinta basin. Immiscible oils generated at equivalent maturity levels by hydrous pyrolysis show significant variability within the same facies of the Green River Formation. An immiscible oil from the upper carbonate marker bed of the upper black shale facies (sample 930923-6) closely resembles immiscible oils from the mahogany shale. These features include a black, liquid, immiscible oil; abundant acyclic isoprenoids and β-carotane; and an odd predominance in the n-alkanes (Figure 10; Table 7). As previously noted, there are no documented crude oils from the Uinta basin at this high level of maturity that have a similar composition. Correlation between immiscible oils from the upper carbonate marker and mahogany shale, however, suggests that either of these units could be the source of the low-maturity crude oils in the Altamont field and elsewhere in the Uinta basin. The organic source material and

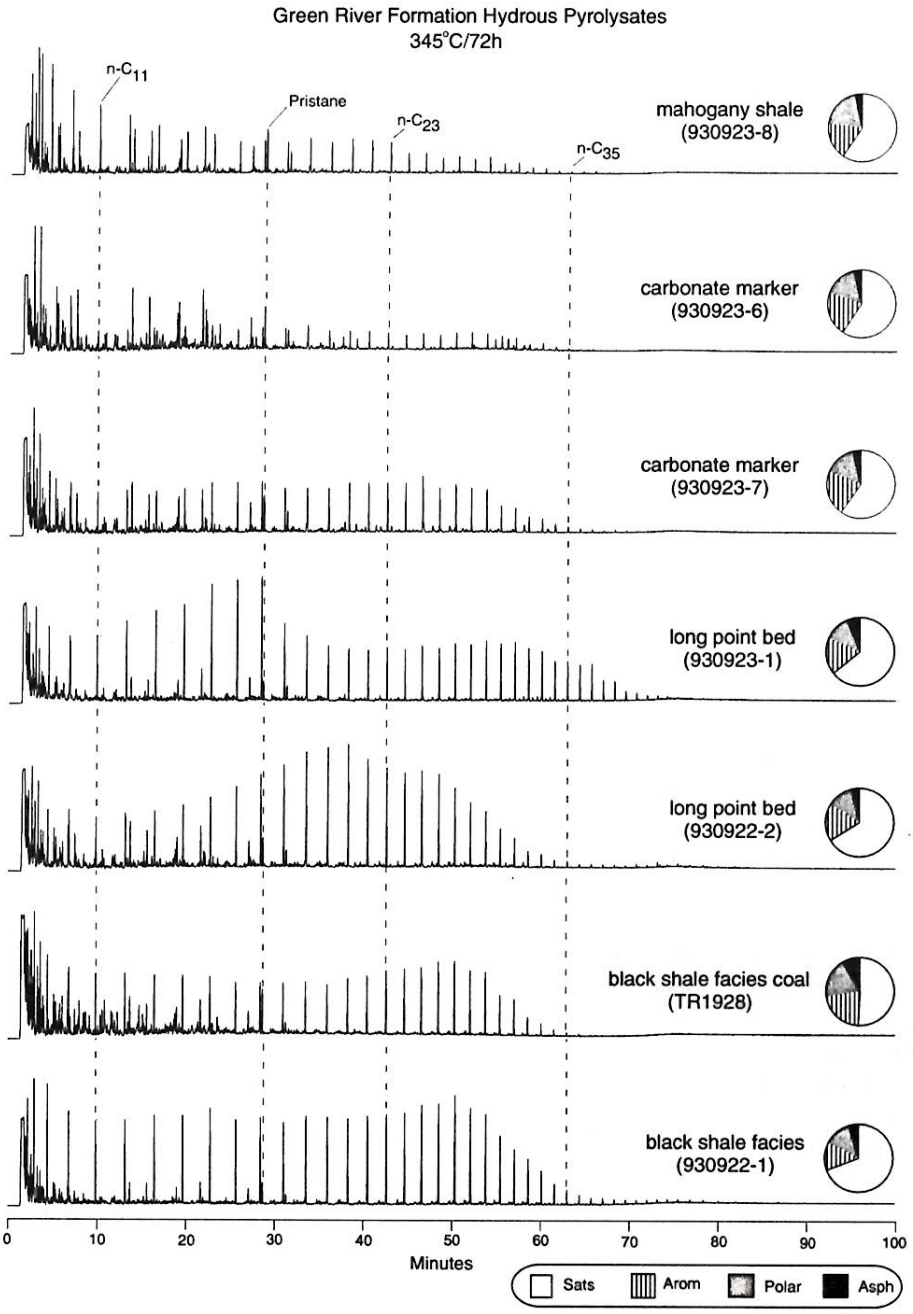

Figure 10. Whole-oil gas chromatograms and fractional compositions for immiscible oils generated during 345°C/72 hr hydrous pyrolysis experiments from various source rock lithofacies collected from the Green River Formation in Indian Canyon. Samples are in stratigraphic order from shallow (top) to deep (bottom). See Table 1 for further details. Conditions of analysis are described by Ruble (1996).

depositional environment (offshore, open lacustrine) for both the mahogany shale and upper carbonate marker source rocks may have extended throughout the main lacustrine depositional phase in the Uinta basin at various paleogeographic locations (Ryder et al., 1976). Therefore, when discussing oil–source rock correlation and the distribution of potential source facies, it is important to recognize that both lateral and vertical variability coexist and that Walther's law of facies (Walther, 1894) applies to the distribution of kerogen types in these lacustrine systems (see Figure 3).

Another immiscible oil generated by hydrous pyrolysis of a source rock from a slightly lower stratigraphic position in the carbonate marker of the upper black shale facies (sample 930923-7) has characteristics of both the mahogany shale and lower black shale

Table 7. Molecular Maturity Ratios in the Immiscible Oils from Various Green River Formation 345°C/72 Hr Hydrous Pyrolysis Experiments*

Maturity Ratio	Mahogany Shale (930923-8)	Carbonate Marker (930923-6)	Carbonate Marker (930923-7)	Long Point Bed (930923-1)	Long Point Bed (930922-2)	Black Shale Facies Coal (TR1928)	Black Shale Facies (930922-1)
CPI 1**	1.34	1.11	1.20	1.10	1.09	1.09	1.05
Pristane/n-C_{17}	1.82	3.02	1.14	0.21	0.45	1.33	0.36
Phytane/n-C_{18}	0.96	1.38	0.77	0.28	0.22	0.37	0.16
C_{29} ααα steranes 20*S*/(20*S* + 20*R*)	0.33	n.d.	n.d.	0.28	0.31	n.d.	0.37
C_{29} steranes αββ/(αββ + ααα)	0.35	n.d.	n.d.	0.36	n.d.	n.d.	0.47

*n.d. = No data.
**Hunt (1979).

facies immiscible oils. This immiscible oil is black, viscous, and waxy but is a liquid at room temperature. Its gas chromatogram is dominated by a bimodal distribution of n-alkanes, including higher molecular weight alkanes greater than C_{30} (Figure 10). The n-alkanes have a slight odd predominance, especially in the higher molecular weight region (Table 7). The relative abundance of acyclic isoprenoids is less than in the mahogany shale immiscible oils but greater than in the other waxy immiscible oil from the black shale facies (sample 930922-1). β-carotane is also present in this immiscible oil, but in lower concentrations compared to the mahogany shale immiscible oil at equivalent maturity. In general, this immiscible oil appears to have been generated from a source facies that contained a mixture of the two end-member type I kerogens characterized in this study. This source facies could represent a transition from offshore, open-lacustrine (mahogany shale/upper carbonate marker) to a nearshore, open-lacustrine source facies (lower black shale facies). Although no crude oils analyzed in this study resemble this immiscible oil, there are published chromatograms of such Uinta basin crude oils. Fouch et al. (1994) examined two moderate temperature, black, paraffinic oils that showed abundant acyclic isoprenoids, β-carotane, and an odd predominance in the higher molecular weight n-alkanes. One of these oils was from the Red Wash field (Red Wash 64164), and the other was from the Bluebell field (Victor Brown 1, 9042 ft [2756 m]) at depths that approximate the upper black shale facies (Fouch et al., 1994).

Two immiscible oils from an organic-rich limestone unit (long point bed) at the base of the upper black shale facies (Figure 2) display unique features compared to the other oil samples in this study. Both of these immiscible oils are dark, solid waxes at room temperature and contain significant acyclic isoprenoids and small amounts of β-carotane. One oil (sample 930923-1) has an unusual bimodal distribution of n-alkanes that shows a strong steplike feature at C_{17}, a secondary maximum at C_{29}, and a slight odd predominance (Figure 10). This irregular alkane distribution is identical with that of a microscale sealed-vessel pyrogram of the Laney shale (Green River Formation) from the Washakie basin, Wyoming (Horsfield et al., 1994). This pattern could result from the cracking of a highly structured, macromolecular precursor at sterically favored positions and is representative of the biomass from an ecologically stressed, alkaline lacustrine environment (Horsfield et al., 1994). A similar but less striking alkane pattern is also present in a Uinta basin crude oil (Roosevelt Ute Tribal C-1, 9906–9954 ft [3019–3034 m]) from a reservoir in the upper Wasatch Formation (Reed and Henderson, 1972). The other immiscible oil generated from this source unit (sample 930922-2) has a unimodal distribution of n-alkanes maximizing at C_{21} and is relatively depleted in the higher molecular weight alkanes typically associated with the other waxy immiscible oils and crude oils (Figure 10).

A coal sample (TR1928) from the lower black shale facies collected at a stratigraphic position slightly above sample 930922-1 represents a unique source facies within the lacustrine depositional system. The dominant macerals in this coal are vitrinite, cutinite, and fluorinite (B. Cardott, 1994, personal communi-

cation) derived from higher plant material, especially palms and ferns (Nichols, 1987). The immiscible oil generated from this source facies is a semisolid reddish brown wax at room temperature. The gas chromatogram of this immiscible oil shows a bimodal distribution of n-alkanes having a secondary maximum at C_{27} and a slight odd predominance (Figure 10). The oil contains significant acyclic isoprenoids and aromatics, but no β-carotane. The Pr/Ph ratio of the oil is much higher (3.89) than any other immiscible oils generated by hydrous pyrolysis in this study. These observations are consistent with previous analyses of attrital coal in the North Horn Formation at Price River Canyon in the southwestern part of the Uinta basin (Fouch et al., 1977). Representative samples of that coal yielded as much as 83 gallons of oil per ton, and extracts were characterized by abundant acyclic isoprenoids, a very high Pr/Ph ratio (6.7–9.0), and an odd-carbon predominance in the n-alkanes (Fouch et al., 1977). Similar results were also reported from analyses of Eocene lacustrine coal samples in the Niland Tongue of the Wasatch Formation, Vermillion Creek basin, Wyoming: Pr/Ph (3.8–6.4), CPI (2.1–2.7), and n-alkane distributions maximizing at C_{29} (Bostick et al., 1987). The absence of natural analogs to the coal-derived immiscible oil in our suite of Uinta basin crude oils suggests that these minor coal deposits are of negligible importance as a source of oil in the Green River petroleum system.

In summary, correlation of the immiscible oils generated by hydrous pyrolysis of Green River lacustrine source facies with representative crude oils supports stratigraphic control on the composition of oils in the Uinta basin. Low-grade oil shales from nearshore open-lacustrine units, such as the basal black shale facies, appear to be the principal source of paraffinic crude oils found at various levels of maturity in the deeper parts of fields, such as Altamont. Organic-rich offshore lacustrine facies, such as the carbonate marker and mahogany shale, generated low-maturity oils, which more closely resemble a bitumen phase as defined within the context of this investigation. Our analysis of a variety of subunits from the black shale facies illustrates the diversity of source rocks in the lacustrine system. Although some facies, such as the paludal coal, are probably not important sources of oil in this petroleum system, a better understanding of facies variability and its relation to petroleum generation will improve our ability to effectively and quantitatively model regional hydrocarbon generation, migration, and accumulation.

Gases

Based on chemical and isotopic composition, Rice et al. (1992) identified two distinct groups of thermogenic gases in the Uinta basin (Figure 11a). The first group of gases is not associated with oil. These gases are produced from reservoirs in the Upper Cretaceous Mesaverde Group and Tertiary Wasatch and Green River formations in the Natural Buttes field. They are characterized by wetness values (C_{2+}) between about 5 and 9%, methane $\delta^{13}C$ values greater than −40‰, ethane $\delta^{13}C$ values greater than −28.5‰, and methane δD values greater than −185‰ and are interpreted to have been generated from type III kerogen in the Cretaceous Mesaverde Group at advanced stages of catagenesis and metagenesis (Rice et al., 1992). The second group of gases is associated with oil produced from Green River Formation reservoirs in the greater Altamont-Bluebell and Red Wash fields. These gases have wetness values ranging from about 2 to 23%, methane $\delta^{13}C$ values less than −46.9‰, ethane $\delta^{13}C$ values less than −34.5‰, and methane δD values less than −228‰, and are interpreted to have been generated at intermediate stages of catagenesis from mainly type I kerogen in the Green River Formation (Rice et al., 1992).

In our investigation, the methane and ethane $\delta^{13}C$ values of the gases generated during hydrous pyrolysis were compared to the suite of Uinta basin natural gases analyzed by Rice et al. (1992) and additional samples from the U.S. Geological Survey Geochemical Database (C. Threlkeld, 1995, personal communication). The gases generated by hydrous pyrolysis include the 72 hr temperature series pyrolysates from both the mahogany shale and black shale facies, as well as gas from the 345°C/72 hr pyrolysis of the black shale facies coal sample. Pyrolysate gases from the three different Green River source facies can be easily distinguished; the gas from the terrigenous-dominated Tertiary coal has heavier (more positive) isotopic values compared to the gases from the lacustrine oil shales (Figure 11a). Gases from both the mahogany shale and black shale facies 72 hr temperature series form tight clusters (Figure 11), indicating little isotopic variability with simulated thermal maturity through the zone of oil generation. Despite their presumed origin for the associated gases in the Uinta basin, none of the pyrolysate gases from the Green River Formation correlate isotopically with either of the two groups of natural gas samples (Figure 11a).

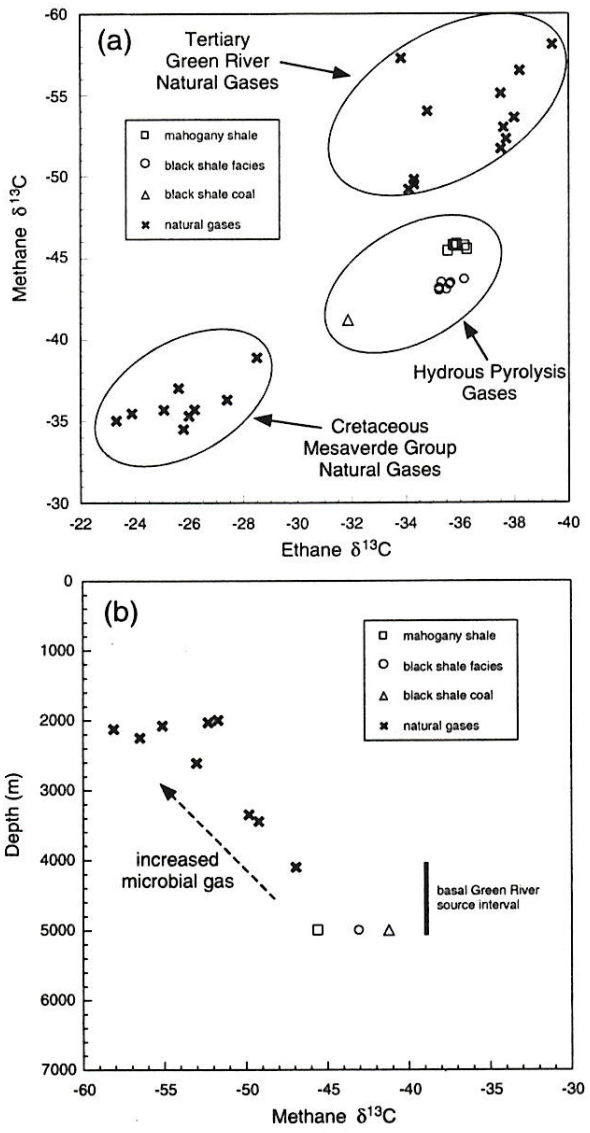

Figure 11. Carbon isotopic compositions of Uinta basin gas samples. (a) Methane $\delta^{13}C$ vs. ethane $\delta^{13}C$ (peedee belemnite per mL) from gases generated during the mahogany shale and black shale facies 72 hr hydrous pyrolysis experiments, the 345°C/72 hr black shale facies coal pyrolysate, and natural gas samples from the Uinta basin (Rice et al., 1992). (b) Depth trend for methane $\delta^{13}C$ of gases from the Altamont field, which are thought to have been mixed with variable amounts of microbial gas (Rice et al., 1992). Average isotopic compositions of the hydrous pyrolysis gases are shown at the approximate depth of the basal Green River source interval in the Altamont field.

One likely explanation for the lack of correlation is apparent on a plot of methane $\delta^{13}C$ vs. depth (Figure 11b), where $\delta^{13}C$ values increase with decreasing depth of production for samples from the Altamont field. Rice et al. (1992) previously noted that shallower gases in this field are drier (C_{2+} values of 3.5 to 13.6%) and have more negative isotopic values for methane, suggesting mixing with variable amounts of isotopically light microbial methane. Where the average isotopic values of the hydrous pyrolysis generated gases are plotted at the general depth of the basal black shale facies productive interval (Figure 11b), the methane $\delta^{13}C$ values fall on the depth trend and appear to represent end-member gases that have not been altered by any input from microbial sources. Because microbial gas is composed primarily of methane, mixtures of isotopically light, dry microbial gas and thermogenic wet gas changes the $\delta^{13}C$ of methane in the mixture to more negative values without changing the $\delta^{13}C$ of ethane (Whiticar, 1994), which is consistent with the data shown in Figure 11a. Thus, it appears that most associated natural gases from the Uinta basin contain some contribution from microbial sources and based on the similarity in ethane $\delta^{13}C$ values and the predicted zones of oil/gas generation, the probable origin of these associated gases are nearshore open-lacustrine source facies in the lower black shale facies.

TIMING OF PETROLEUM GENERATION

Hydrous Pyrolysis Isothermal Kinetics

Theory

Chemical kinetics have been applied to the process of petroleum generation by means of various laboratory simulation techniques (e.g., Snowdon, 1979; Waples, 1984; Sweeney et al., 1987; Lewan, 1992). Hydrous pyrolysis is a particularly useful analog because the products generated are similar to crude oils (Lewan et al., 1979), and kinetic parameters provide reasonable extrapolations into natural systems (Hunt et al., 1991). Simulation of the catagenesis of organic matter by hydrous pyrolysis involves long reaction periods and slow reaction rates of geological processes being replaced in the laboratory with short-time experiments at higher temperatures. Previous studies suggest that although thermal alteration of organic matter may proceed through a complex series of parallel or consecutive chemical reactions, the overall process of immiscible oil generation in hydrous pyrolysis can be described by simple pseudo–first-order reaction kinetics (Lewan, 1985) controlled by initiating free radicals (Lewan,

1998). The chemical kinetic parameters calculated in this manner for high-temperature pyrolysis experiments can then be extrapolated to low-temperature geological systems using the Arrhenius equation,

$$k = Ae^{-E/RT}$$

which expresses the relation between the reaction rate constant (k) and absolute temperature (T); R is the gas constant, E is the activation energy, and A is the frequency factor.

In our hydrous pyrolysis system we distinguish four organic phases: (1) hydrocarbon gases, (2) immiscible oil, (3) extractable bitumen, and (4) kerogen (Figure 4). The interrelation among the four organic phases can be described in terms of three consecutive irreversible pseudo–first-order reactions:

$$A \rightarrow B \rightarrow C \rightarrow D$$

where A is kerogen, B is bitumen, C is immiscible oil, and D is gases.

The system can then be simplified by focusing solely on the pseudoreaction of primary interest to petroleum geochemists, the formation of oil from bitumen. By properly choosing the conditions of the experiments it is possible to consider this pseudoreaction in isolation. Previous hydrous pyrolysis kinetic parameters were determined in this manner (e.g., Lewan, 1985), by considering the bitumen to oil conversion as a simple pseudo–first-order reaction of the type:

$$B \rightarrow C \text{ rate constant } = k$$

where the differential rate equation is

$$-\left(\frac{dc_B}{dt}\right) = kc_B$$

the integrated rate equation is

$$\ln\left(\frac{c_{oB}}{c_B}\right) = kt$$

and the modified rate equation used for analysis of hydrous pyrolysis data is

$$\ln\left[\frac{1}{(1 - X)}\right] = kt$$

determined by setting the initial concentration $c_{oB} = 1$ and defining $c_B = (1 - X)$, where X is the fraction of maximum immiscible oil generated.

The rate constant (k) at a given temperature may be calculated as the slope of a plot of $\ln[1/(1 - X)]$ vs. time, provided that this calculation is performed in the linear region of such a plot where the pseudoreaction is behaving in a first-order manner.

Quantitative yields of the immiscible oils generated (Tables 2, 3) were converted to fractions of the maximum of oil generated (X), and the values of $\ln[1/(1 - X)]$ were plotted vs. time (Figure 12). The maximum immiscible oil yields (oil/rock) used to calculate X were 90.42 mg/g for the mahogany shale (360°C/96 hr) and 32.33 mg/g for the black shale facies (365°C/72 hr). Rate constants (k) for each time series were determined from linear regressions through all

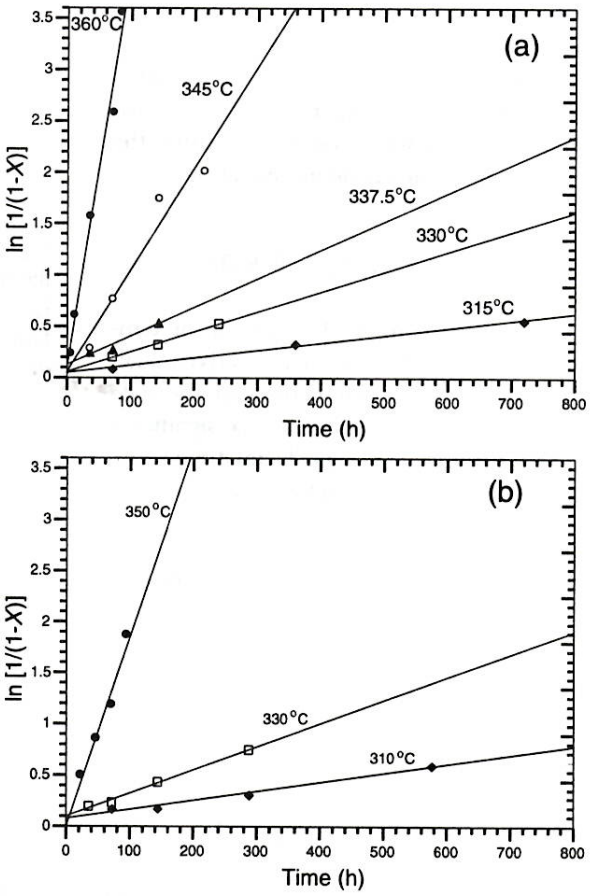

Figure 12. Plots of $\ln[1/(1 - X)]$ vs. time for the immiscible oils generated by hydrous pyrolysis of (a) mahogany shale and (b) black shale facies (X = fraction of maximum immiscible oil generation). Data from linear regression are in Table 8.

the isothermal data points (Table 8). To maximize the number of data points, rate data from both Green River source facies were applied to a single Arrhenius plot of $\ln(k)$ vs. $1/T$ (Figure 13). Although there are distinct differences in the molecular composition of the immiscible oils generated from the mahogany shale and black shale facies source rocks, the similarity in their gross composition (Figure 5) and generation curves suggest that both type I kerogens have comparable oil-generation kinetics. The E and A values were determined from the respective slope and intercept of a linear regression through the valid data points. More hydrous pyrolysis time-series experiments were conducted on the mahogany shale (315, 330, 337.5, 345, and 360°C) than on the black shale facies (310, 330, and 350°C), which is reflected in the number of data points on the Arrhenius plot. The mahogany shale was chosen for more detailed study because its widespread use in previous kinetic investigations (e.g., Leavitt et al., 1987; Sweeney et al., 1987) allows comparison of our kinetic data with those of others.

As a measure of the consistency of the calculated kinetic parameters with the experimental data, synthetic generation curves were constructed using the following expression of the Arrhenius equation:

$$X = 1 - \exp(-tA \exp(-E/RT))$$

These curves were compared to the 72 hr temperature series experimental data in a sensitivity analysis during which various combinations of the data were evaluated. These analyses reveal a significant anomaly in the 310°C black shale facies time-series data, and this data point was therefore excluded from

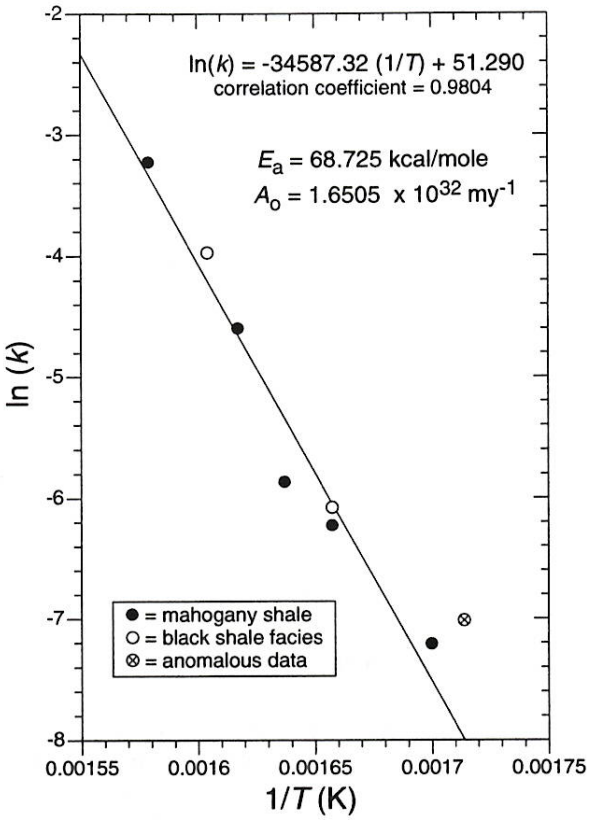

Figure 13. Arrhenius plot of the $\ln(k)$ vs. 1/temperature for the immiscible oils generated by hydrous pyrolysis of Green River samples from both the mahogany shale and black shale facies. Rate constants (k) were determined using the data shown in Figure 12. The activation energy (E_a) and frequency factor (A_o) were determined from the respective slope and intercept of a linear regression line through the data points (Table 8). The black shale facies 310°C data point (⊗) was not included in the calculated linear regression (see text and Figure 14).

Table 8. Linear Regression Equations for Hydrous Pyrolysis Kinetic Data in Figures 12 and 13

Sample	Temp. Series (°C)	Number of Data Points	Linear Equation	Correlation Coefficient
Mahogany shale	360	5	$f(x) = (3.897425 \times 10^{-2}x) + (8.297712 \times 10^{-2})$	0.9901
Mahogany shale	345	4	$f(x) = (9.907918 \times 10^{-3}x) + (4.885629 \times 10^{-2})$	0.9700
Mahogany shale	337.5	3	$f(x) = (2.787202 \times 10^{-3}x) + (1.184921 \times 10^{-1})$	0.9694
Mahogany shale	330	3	$f(x) = (1.946170 \times 10^{-3}x) + (4.967331 \times 10^{-2})$	0.9974
Mahogany shale	315	3	$f(x) = (7.283725 \times 10^{-4}x) + (4.175752 \times 10^{-2})$	0.9965
Black shale facies	350	4	$f(x) = (1.849479 \times 10^{-2}x) + (-1.946090 \times 10^{-2})$	0.9830
Black shale facies	330	4	$f(x) = (2.257253 \times 10^{-3}x) + (9.171435 \times 10^{-2})$	0.9970
Black shale facies	310	4	$f(x) = (8.839723 \times 10^{-4}x) + (6.963660 \times 10^{-2})$	0.9902
Green River shale	Arrhenius equation	8	$f(x) = (-3.458732 \times 10^{4}x) + (5.128967 \times 10^{1})$*	0.9804

*Time units in this equation are in hours.

the final linear regression on the Arrhenius plot (Figure 13). This anomaly is apparently a consequence of enhanced yields of low-temperature (<330°C) immiscible oil generated during hydrous pyrolysis of the black shale facies source rock (Figure 14b) and may be related to the specific physical characteristics of the waxy pyrolysates produced from this source facies. Highly aliphatic bitumens may promote earlier phase separation and expulsion of the immiscible oil from the water-saturated bitumen phase. Exclusion of this data point gives a linear Arrhenius plot ($r = 0.98$), having an activation energy of 68.7 kcal/mole and a frequency factor of 1.65×10^{32} m.y.$^{-1}$. Generation curves constructed from these kinetic parameters closely match the data from the main zone of immiscible oil generation in both the mahogany shale and black shale facies 72 hr temperature series experiments (Figure 14), and it is these composite closed-system kinetic parameters that were applied to model oil generation from Green River source rocks in the Uinta basin.

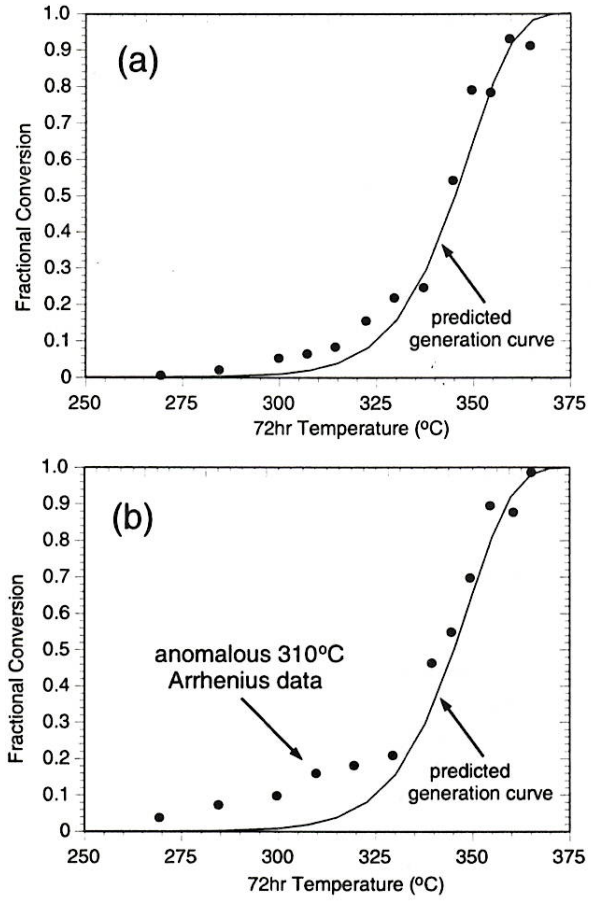

Figure 14. Comparison of the fractional conversion (X) vs. temperature using the 72 hr hydrous pyrolysis data points and generation curves constructed using the kinetic parameters calculated from the Green River time-temperature series hydrous pyrolysis data (Figures 12, 13). The curves were constructed using a modified Arrhenius equation, where the fractional conversion $X = 1 - \exp[-tA \exp(-E/RT)]$. Figures illustrate that (a) mahogany shale data points generally follow predicted generation curve, whereas (b) low-temperature black shale facies data points diverge from the predicted curve and were thus excluded from the determination of Arrhenius constants (Figure 13).

Basin Predictions

The kinetic parameters for immiscible oil generation determined by hydrous pyrolysis were applied to a burial model of the Uinta basin using BasinMod 1-D for Windows Version 5.4 (from Platte River Associates, Denver). Many previous studies used the Shell 1-11-B4 Brotherson well to model hydrocarbon generation in the Uinta basin (Sweeney et al., 1987; Anders et al., 1992; Bredehoeft et al., 1994; Fouch et al., 1994; McPherson, 1996). This oil well is one of the deeper, but not the deepest drilled in the northern margin of the basin along the Altamont/Bluebell trend (Figure 1), and it was selected for use in our study because its depositional history is well known, and the well produces from deeply buried (3500–4500 m), overpressured strata associated with lacustrine source rocks in the basal Green River Formation (Fouch, 1981). The input parameters for the current model are based upon those used by Fouch et al. (1994) but were modified to reflect our best estimates of overburden removal and geothermal gradient (Table 9). The burial history curve (Figure 15) was reconstructed using formation thicknesses from geophysical logs (Fouch et al., 1994), and we assumed that 1796 m of post–Duchesne River Formation (30 to 10 Ma) was eroded between 10 Ma and the present, as determined by Sweeney et al. (1987). The thermal history is based on a geothermal gradient of 25°C/km and an ambient surface temperature of 10°C (Anders et al., 1992). Although there is still controversy regarding the estimated amounts of erosion in this area (see McPherson [1996] for discussion), all geological parameters were held constant for the models used in our investigation because our goal was to examine the variability imposed by different kinetic input parameters.

The results of the hydrous pyrolysis kinetic model for the Shell 1-11-B4 Brotherson well show that generation of oil from the Green River Formation was restricted to units below the carbonate marker horizon (> 3200 m), which includes the main basal source pod

Table 9. Events Chart for Uinta Basin Burial History Used in the Basin Models in Figure 15

Event	Time Period (Ma)	Thickness (m)
Erosion	10–present	−1796
Hiatus	20–10	-
Uinta and Duchesne River formations and Bishop Conglomerate	37–20	1677.5
Upper Green River Formation (undifferentiated)	43–37	762.5
Mahogany bed	45–43	30.5
Parachute Creek Member and upper black shale facies	53–45	854
Carbonate marker	54–53	30.5
Green shale facies and Flagstaff Formation Lower black shale facies (part)	58.3–54	854
Lower marker	58.3	-
Lower black shale facies (part) Flagstaff and North Horn formations (part)	66–54.0	854
Paleocene–Cretaceous boundary	66	-

within the Flagstaff Member and lower black shale facies (Figure 15). Hydrous pyrolysis kinetics predict that the generation of an expelled oil began near the base of the Green River Formation around 25 Ma during rapid subsidence to maximum burial. Potential source rocks within this basal pod are thought to have undergone no more than 85% fractional conversion at this locality. The upper part of the basal source rock section is at less than 10% fractional conversion (Figure 16). This remaining source potential indicates that significant petroleum formation may be active today in more deeply buried regions of the source kitchen north of the Shell 1-11-B4 Brotherson well site. The variable transformation ratios predicted by this model for the basal source pod are consistent with the occurrence of natural paraffinic crude oils of variable maturity in the deep Altamont field. As discussed previously, correlation of such natural crude oils with the suite of immiscible oils from the black shale facies indicates that the natural paraffinic oils bracket a maturity range from incipient to peak oil generation.

Deeply buried reservoirs in the Altamont oil field are known to have pore pressures approaching 80% of lithostatic pressure (Lucas and Drexler, 1975; Bredehoeft et al., 1994). Permeability in these reservoir rocks is thought to result from high pore-pressure fractures (Bredehoeft et al., 1994; Fouch et al., 1994). No cap rock and no trap exists as in most oil reservoirs. One explanation for the occurrence of these overpressured reservoirs is active oil generation from source beds in the basal Green River Formation (Bredehoeft et al., 1994). Our results using hydrous pyrolysis–derived kinetic parameters are consistent with this mechanism for overpressuring. A comparison of the actual fluid pressures vs. depth for the Shell 1-11-B4 Brotherson well (Figure 17) shows a good correlation between the observed high pressured zone (3000–5000 m), the oil-producing interval (3500–4500 m), and the zone of oil generation predicted in the hydrous pyrolysis basin model (>3200 m). In addition, the predicted zone of oil generation also corresponds to a kink in the vitrinite reflectance profile for this well between about 3800 and 4900 m (Figure 17). This discontinuous vertical reflectance profile is thought to represent either a perturbation of heat transfer associated with the zone of overpressuring and hydrocarbon generation (Law et al., 1989) or a suppression of the vitrinite kinetic reaction within the overpressured system (Fouch et al., 1994). The kink in the vitrinite reflectance profile in this well occurs at % $R_o \approx 1.0$, which we suggest represents maturity equivalent to peak oil generation for these lacustrine source rocks. This proposed maturity is at the high end of the range established for peak oil generation, about 0.8–1.0% R_o (e.g., Peters and Moldowan, 1993), but generation from these low-sulfur type I kerogens is typically delayed compared to other kerogen types. For example, Baskin and Peters (1992) report the onset of oil generation from Green River Shale does not occur until % $R_o \approx 0.75$, which is also consistent with zone of oil generation predicted using the hydrous pyrolysis kinetic model (Figure 17).

From all of the empirical evidence available, it appears that hydrous pyrolysis kinetic parameters for immiscible oil generation are generally consistent with both the experimental and the observed natural data. Our basin model suggests that there is sufficient generative potential remaining in the basal Green River source kitchen to allow active oil generation to account for overpressuring in the deep Uinta basin reservoirs. As discussed in the following section, this is a problem with other basin models that use open-system pyrolysis kinetics, because the geothermal gradient and/or permeability parameters in these models must be lower than measured data to sustain overpressure (Bredehoeft et al., 1994).

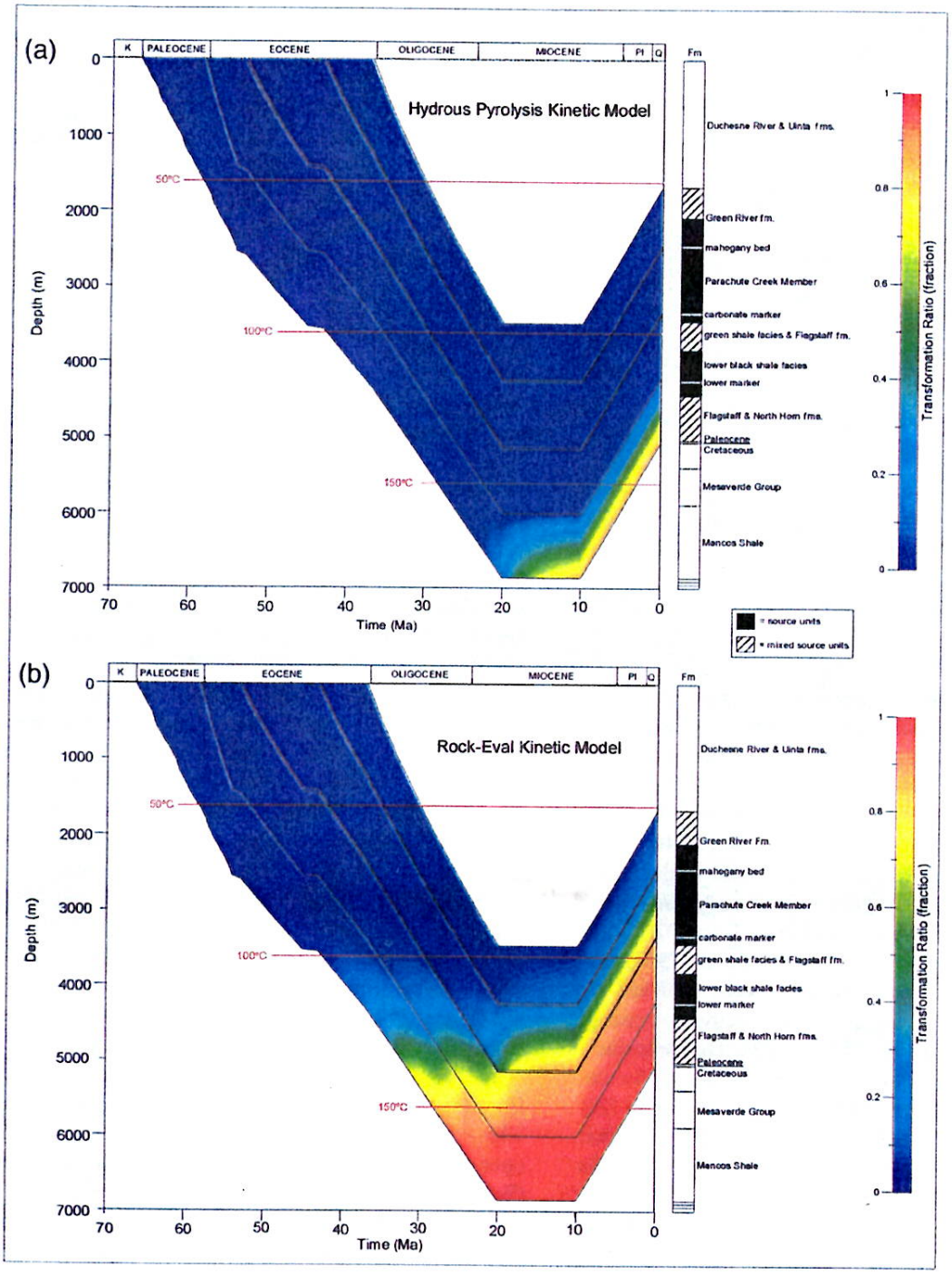

Figure 15. Burial history curves and kinetic models for the Shell 1-11-B4 Brotherson well in the Altamont field. Burial history (Table 9) was reconstructed using formation thicknesses from geophysical logs. The models assume a geothermal gradient of 25°C/km, an ambient surface temperature of 10°C, and 1796 m of overburden removal. (a) Results using hydrous pyrolysis–derived kinetic parameters. (b) Rock-Eval kinetic parameters (mahogany shale above the carbonate marker and black shale facies below this marker). The nature and location of the source rocks are illustrated in the stratigraphic log adjacent to each model.

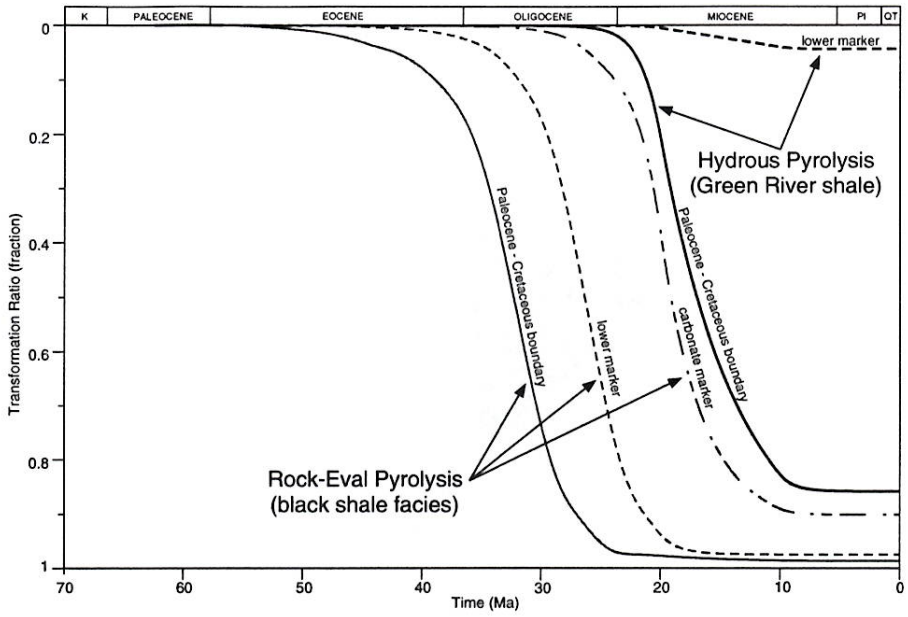

Figure 16. Comparison of the predicted timing of generation in the Shell 1-11-B4 Brotherson well from various marker horizons in the basal Green River source pod for the hydrous pyrolysis and Rock-Eval kinetic models. Marker horizons are illustrated in the stratigraphic cross section in Figure 2.

Rock-Eval Nonisothermal Kinetics

Rationale

Nonisothermal open-system pyrolysis was also used to determine kinetic parameters for hydrocarbon generation from the mahogany shale and black shale facies source rocks. Such methods were used in previous attempts to model hydrocarbon generation in the Uinta basin (e.g., Sweeney et al., 1987). Table 10 shows some of the kinetic parameters reported in the literature using these techniques. In our study two Green River source rocks were heated at 1, 5, and 32°C/min using a Rock-Eval 5 instrument (D. Jarvie, 1994, personal communication). The data were analyzed by nonlinear regression using a discrete activation energy model (Burnham et al., 1987, 1988). This procedure results in a distribution of activation energies and a single frequency factor for each source rock (Figure 18), which describe the series of reactions during thermal degradation of kerogen under open-system anhydrous pyrolysis conditions. Activation energies for the mahogany shale show a narrow distribution, and greater than 80% of the reaction has an activation energy of 51 kcal/mol. This narrow activation energy distribution is typical of Green River shale (Table 10), which contains a relatively homogeneous kerogen composition (Schenk et al., 1997). In contrast, the black shale facies source rock has a lower maximum and much broader distribution of activation energies (Figure 18), consistent with a more heterogeneous kerogen composition as observed in the alkaline Laney shale member of the Green River Formation in the Washakie basin, Wyoming (Schenk et al., 1997).

Kinetic parameters determined by open-system methods measure products released during high temperature (210–550°C) anhydrous pyrolysis of the source rock. As a consequence of the experimental design, open-system kinetic parameters fail to differentiate between the various organic phases and are a measurement of all volatilized organic products. For low-sulfur Green River kerogen, the distribution of activation energies determined by open-system methods are significantly lower than the single activation energy value determined using closed-system hydrous pyrolysis (Figure 18). This is likely due to the inclusion of a large bitumen and gas component in the kinetic parameters determined by open-system pyrolysis methods (Lewan, 1993). Evidence of this is shown in Figure 5, where the composition of the C_{15+} pyrolysate from open-system pyrolysis of type I Green River kerogen (Behar et al., 1997) is plotted on a ternary diagram. The composition of this open-system pyrolysate resembles neither natural crude oils nor the immiscible oils generated by hydrous pyrolysis but is more similar to natural and experimentally derived bitumens. As documented in the following section, the differences in kinetic parameters as determined by the Rock-Eval methodology can have a significant effect on the predicted location, timing, and rates of oil generation in the Uinta basin.

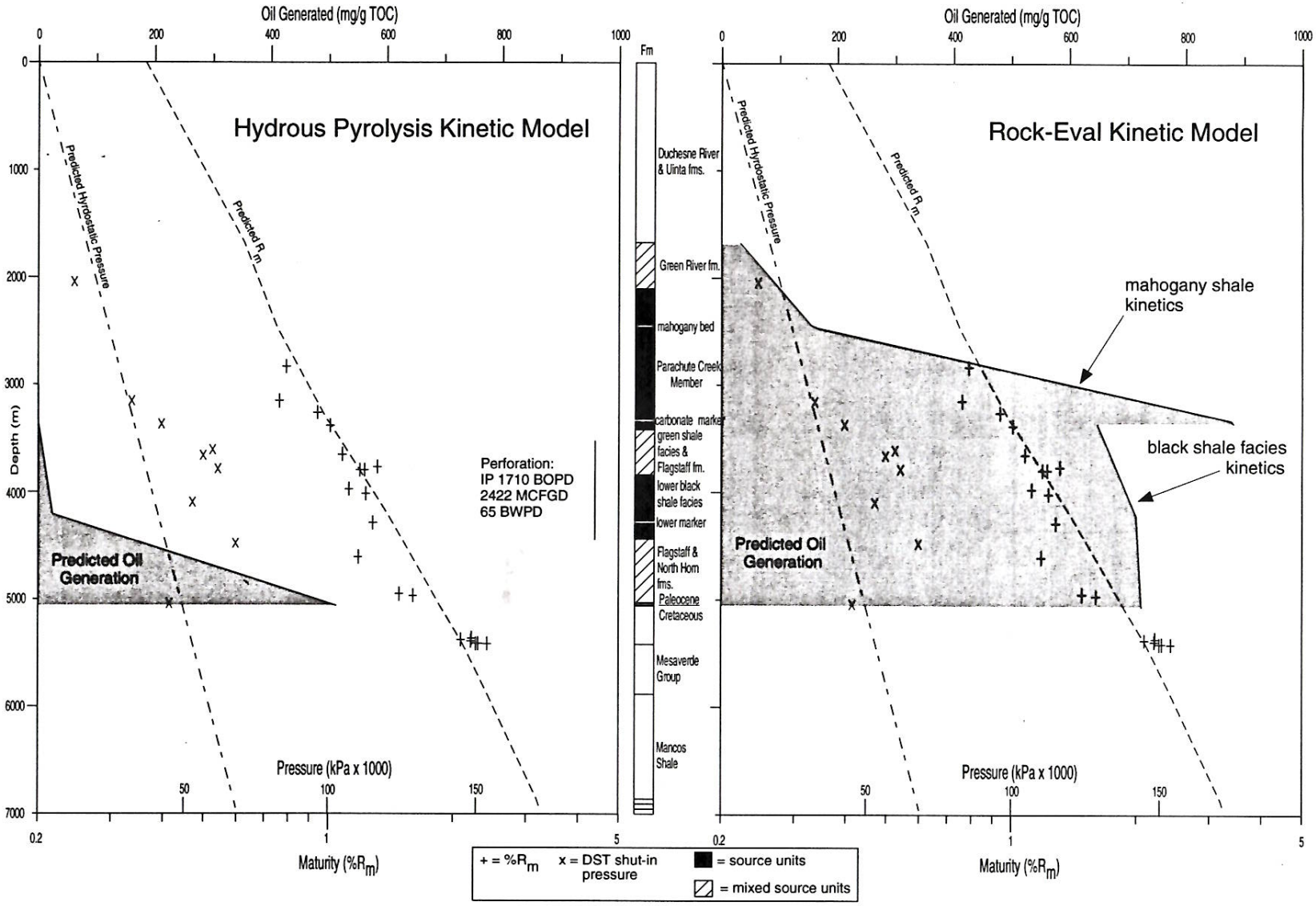

Figure 17. Predicted zones of oil generation in the Shell 1-11-B4 Brotherson well compared to the perforated production interval and the measured zones of overpressuring and vitrinite reflectance suppression. Note the general overlap of these zones in the hydrous pyrolysis kinetic model (left) in contrast to the Rock-Eval kinetic model (right). Initial production values shown refer to barrels of oil per day (BOPD), million cubic feet of gas per day (MCFGD), and barrels of water per day (BWPD).

Table 10. Comparison of Kinetic Parameters from this Study and the Literature for Green River Samples*

Study	Method	Unit/Location	Activation Energy (kcal/mole)	Frequency Factor ($m.y.^{-1}$)
Current study	hydrous pyrolysis	Green River shale/Uinta basin, UT	68.7	1.7×10^{32}
Huizinga et al. (1988)**	hydrous pyrolysis	Green River shale/Piceance basin, CO	67.8	3.5×10^{32}
Current study	Rock-Eval 5	mahogany shale/Uinta basin, UT	53–51†	3.8×10^{26}
		black shale facies/Uinta basin, UT	52–48†	1.1×10^{26}
Burnham et al. (1996)	fluidized-bed	Green River shale/Piceance basin, CO	56.9	2.2×10^{28}
	Pyromat 2	Green River shale/Piceance basin, CO	54.3	3.5×10^{27}
Sweeney (1988)	Rock-Eval	mahogany shale/Uinta basin, UT	50.7	1.8×10^{26}
		black shale facies/Uinta basin, UT	48.0	6.0×10^{25}
Burnham et al. (1987)	Rock-Eval 2	Green River shale/Piceance basin, CO	53–51†	6.9×10^{26}
Sweeney et al. (1987)	Rock-Eval	Green River shale/Piceance basin, CO	52.4	distribution
Shih and Sohn (1980)	modified Fisher Assay	Green River shale/Piceance basin, CO	47.7	2.6×10^{25}
Campbell et al. (1978)	modified Fisher Assay	Green River shale/Piceance basin, CO	52.4	8.8×10^{26}
Braun and Rothman (1975)	modified Fischer Assay	Green River shale/Piceance basin, CO	42.4	6.3×10^{23}

*Green River Shale samples analyzed from the Piceance basin, Colorado, in previous studies are from a stratigraphic equivalent of the mahogany shale bed.
**Temperature series data presented in this study were used to determine kinetic values.
†Range of activation energy distribution representing ≥ 89% of the reaction.

Basin Predictions

The kinetic parameters determined by Rock-Eval pyrolysis of the mahogany shale and black shale facies source rocks were incorporated into a model of hydrocarbon generation for the Uinta basin. The same input parameters from the Shell 1-11-B4 Brotherson well

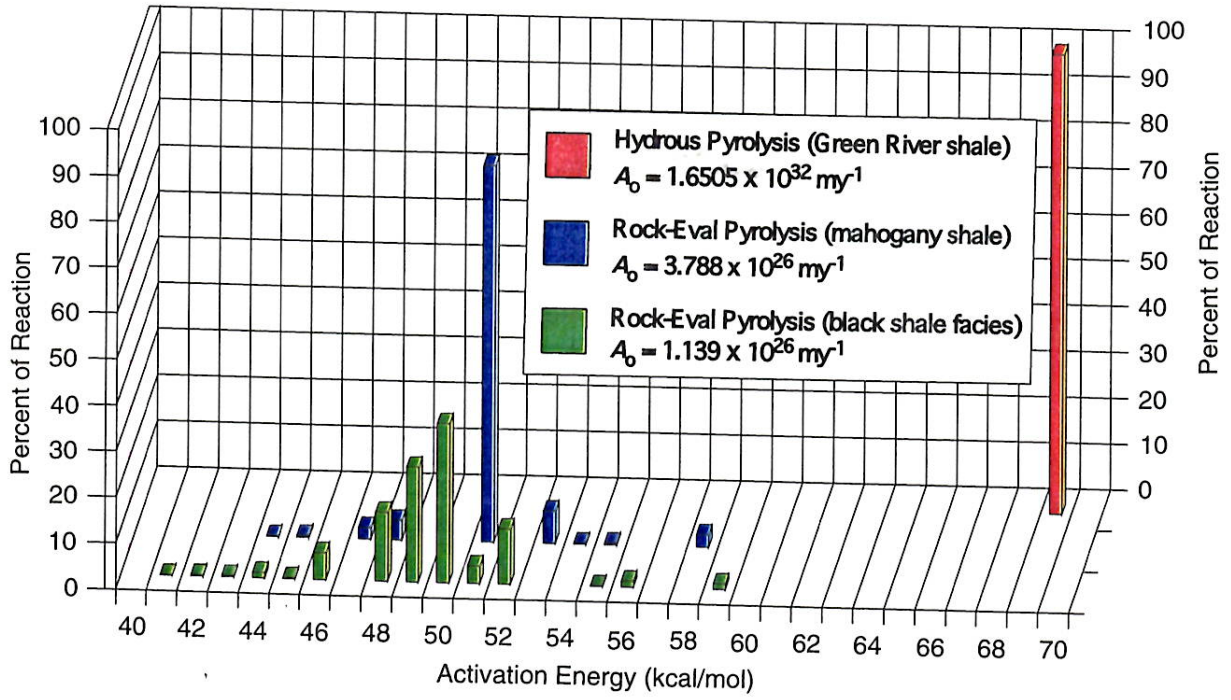

Figure 18. Histograms show the distribution of activation energies (E_a) for the mahogany shale and black shale facies source rocks as determined by Rock-Eval pyrolysis (associated frequency factors, A_o, are in the legend). Kinetic parameters determined by hydrous pyrolysis are also shown for comparison.

were used, except for the revised kinetic values and generative potential associated with the two source rocks. The Rock-Eval kinetic parameters from the mahogany shale and black shale facies were used for the upper (carbonate marker and above) and basal source rock sections, respectively. This assignment is based on crude oil–immiscible oil correlations performed on various Green River source rocks, suggesting a change in the composition of the organic matter above and below this marker horizon.

Unlike the hydrous pyrolysis kinetic model, source rocks in both the upper and the basal Green River sections are predicted to have generated hydrocarbons in the Rock-Eval kinetic model (Figure 15). The Rock-Eval model suggests that hydrocarbon generation began near the base of the Green River Formation around 50 Ma at a depth of about 3000 m. The basal source rock pod is predicted to have passed through the main stage of oil generation during rapid burial to maximum depth between 20 and 40 Ma. Rates of hydrocarbon generation in the basal Green River Formation during this period were extremely high, as was the conversion of the organic matter measured by the transformation ratios (Figure 16). The main pod of source rocks in the basal section had undergone almost complete fractional conversion by 20 Ma, as illustrated by transformation ratios for the lower marker horizon (Figure 16). By 15 Ma the entire basal source rock section below the carbonate marker horizon is predicted to have undergone greater than 90% fractional conversion (Figure 16). The Rock-Eval kinetic model suggests that oil in the lower part of the Green River Formation was cracked to gas and condensate beginning about 30 Ma. Because present-day oil generative potential is exhausted in the basal source rock section, active gas generation is the presumed explanation for the zones of overpressure and vitrinite reflectance suppression in the Rock-Eval model (Figure 17). The difficulty with this explanation is that wet-gas generation is likely to have been most active prior to erosion, during the hiatus of maximum burial (20–10 Ma) when paleoformation temperatures are estimated to have been greater than 150°C (Figure 15). Previous basin models attempted to compensate for this difficulty by assuming higher geothermal gradients and no erosion in the Shell 1-11-B4 Brotherson well (Fouch et al., 1994), resulting in much higher predicted present-day formation temperatures consistent with active gas generation. Measured DST temperatures from this well, however, are inconsistent with such models and show that even at 5000 m depth, the present-day temperatures are less than 150°C (Wesley, 1990; Bredehoeft et al., 1994).

The Rock-Eval kinetic model also indicates that significant hydrocarbon generation occurred in the main source rock sequence of the upper Green River Formation (Figure 17). Generation began around 30 Ma in the carbonate marker horizon, and by the start of the erosional event at 10 Ma the zone of hydrocarbon generation rose to above the mahogany bed (Figure 15). Predicted transformation ratios in the upper Green River Formation range from about 20% in the mahogany bed to about 90% at the carbonate marker. Because of the slightly different input parameters for generative potential and kinetics, oil generation from the lower Parachute Creek Member and from the carbonate marker horizon in the upper black shale facies is predicted to be slightly greater than for the more mature pod of basal Green River source rocks beneath this horizon (Figure 17). The predicted oil generation shown in Figure 17 represents total products generated and does not include a compensation factor for initial hydrocarbon saturation prior to expulsion. Use of such an expulsion saturation factor was deemed inappropriate for the hydrous pyrolysis kinetic model because it is based on experimental measurements of expelled immiscible oil and on the tenet that oil generation and expulsion are coupled. Because the goal of this study was to directly compare the two different kinetic models, such expulsion saturation factors were not used in the Rock-Eval model either, and, had they been used, predicted amounts and timing of oil generation would have changed very little. This is because saturation thresholds in organic-rich oil-prone lacustrine carbonates, such as the Green River Formation, are typically very low and oil expulsion should commence after a minimum fraction (<20%) of the labile kerogen has degraded (Pepper, 1991).

Hydrocarbon generation from the upper Green River source facies is supported to some extent by observed data. The Shell 1-11-B4 Brotherson well (Figure 17) shows anomalously high DST pore pressures beginning at depths near 3000 m. In contrast to the hydrous pyrolysis kinetic model, the Rock-Eval model suggests that the increase in pore pressures is not coincident with the initiation of oil generation but occurs at a higher maturity that might account for the buildup of pressure. Furthermore, vitrinite reflectance data from this well (0.79 R_o; 2835 m) suggest that the upper Green River source rocks are in the oil-generation window (>0.7 R_o), albeit above the kink in the reflectance profile (Anders et al., 1992; Fouch et al., 1994).

Biomarker maturity data from core samples in the Altamont-Bluebell field are generally consistent with the vitrinite reflectance data (Mueller, 1998). Most hopane and sterane maturity parameters indicate that source rocks below the middle marker horizon (~2835 m in the Shell 1-11-B4 Brotherson well) are entering the oil-generation stage (Mueller, 1998). Biomarker evidence also suggests that the mixed fluvial/alluvial section (green shale facies, Flagstaff formation, Colton Formation) that separates the upper and basal Green River Formation are not at peak oil generation (Mueller, 1998).

Perhaps the most compelling evidence for oil generation from the upper Green River Formation is documentation of shallow oil shows in the Shell 1-11-B4 Brotherson well at about 2000 m (Fouch, 1981). Although the presence of such oil shows seems to provide conclusive evidence in support of the Rock-Eval kinetic model, it is not uncommon to find shows throughout the organic-rich source rock sequence, even in areas where the source rocks are immature with respect to oil generation. Caution should be exercised in regard to these shallow shows until detailed geochemical analyses are performed because these oils may represent expelled bitumens, or they may be oils that have migrated through open fractures from more deeply buried source facies.

Compared to hydrous pyrolysis kinetic parameters, Rock-Eval kinetics predict the onset of hydrocarbon generation in the Uinta basin earlier and at shallower depths. This is due to fundamental differences between the experimental procedures. Rock-Eval measures total hydrocarbon generation (bitumen + oil + gas), whereas hydrous pyrolysis distinguishes each organic phase and measures the kinetics of oil generation (Lewan, 1993). One of the difficulties previously encountered in basin models using Rock-Eval kinetics is that hydrocarbon generation occurs too early and too quickly during rapid burial to account for the overpressured reservoirs in the Uinta basin (Bredehoeft et al., 1994). This is because in such models there is a large pulse of generation during rapid burial 20–40 Ma, followed by a rapid decline in generation from 20 Ma to the present, when the overpressure can dissipate. To sustain overpressure conditions in the deep reservoirs for periods over a few hundred thousand years using this model, one must reduce the regional geothermal gradient from 25 to 22°C/km, decrease the rock permeabilities by four orders of magnitude, and disregard 1.8 km of eroded section (Bredehoeft et al., 1994). No evidence exists to support such extreme alterations to the geological data. Alternatively, the results of the two models presented in this study suggest that transformation ratios may be lower and rates of recent oil generation may be higher in the basal Green River Formation when using hydrous pyrolysis rather than conventional Rock-Eval kinetic parameters. Although our revised kinetic parameters may not eliminate all of the difficulties encountered in the previous models, hydrous pyrolysis kinetics provide more realistic conditions from which other variables may be evaluated.

CONCLUSIONS

The quantitative hydrous pyrolysis data from this study provide a useful means to evaluate compositional variations in the products from highly aliphatic type I lacustrine organic matter with thermal maturity. These data also offer insights into the physiochemical processes occurring during hydrous pyrolysis and support the previously suggested stages of hydrocarbon generation: (1) bitumen and (2) immiscible oil, followed by (3) gas and pyrobitumen (Lewan, 1994). The presence of an intermediate bitumen phase is critical to compare our experimental results to the natural system because formation of a saturate-rich immiscible oil analogous to natural crude oils requires phase separation of the oil from the polar-rich, water-saturated bitumen phase within the source rock. These processes operate in closed-system hydrous pyrolysis, but they do not occur in open-system pyrolysis. Quantitative fractional yields indicate that saturated hydrocarbons in oil originate mainly from asphaltenes in the bitumen. These data further suggest that most polar and aromatic components originate from the kerogen during maturation and that these fractions are not significantly involved in the phase separation of oil from bitumen. Ternary diagrams of fractional composition of the immiscible oils and bitumens generated by hydrous pyrolysis clearly distinguish these two organic phases. Waxy immiscible oils generated from the black shale facies are similar to paraffinic Uinta basin crude oils, but are relatively enriched in aromatics. Low-maturity aromatic-intermediate and aromatic-asphaltic oils from the Uinta basin are interpreted to represent expelled bitumens, based on hydrous pyrolysis experiments. These observations offer additional insights into the probable origin of such low-maturity samples, which have also been reported in other lacustrine basins worldwide.

Our hydrous pyrolysis experiments allowed correlation of crude oils and natural gases in the Uinta basin with their respective source rocks. This approach eliminates the facies variability typically associated with natural suites of source rocks and offers the opportunity to examine source- and maturity-related parameters independently. Aromatic-intermediate oils from shallow reservoirs in the Altamont field correlate with pyrolysates from the type I kerogen in offshore open-lacustrine source rocks like the mahogany shale and upper carbonate marker horizons of the Green River Formation. These oils have characteristic features, such as abundant acyclic isoprenoids and β-carotane, and n-alkanes that have a strong odd predominance. Maturity-dependent molecular parameters suggest that these relatively shallow oils are low maturity and correlate with the maximum in bitumen generation observed during hydrous pyrolysis (330°C/72 hr). High-maturity immiscible oils from pyrolysis of offshore open-lacustrine oil shales do not correlate with known crude oils, confirming that this type of kerogen is not the source of waxy crude oils produced from deeper reservoirs in the Uinta basin.

The immiscible oils generated by hydrous pyrolysis of the basal Green River black shale facies correlate well with the deeper crude oils from the Altamont field. These samples are solid waxes at room temperature and are dominated by n-alkanes having no odd-even predominance, including high molecular-weight species greater than C_{40}. Acyclic isoprenoid concentrations are low in these samples and they contain no β-carotane. Maturity/depth trends shift the bimodal distribution of alkanes to lower molecular weight and decrease isoprenoid/alkane ratios. Molecular maturity parameters suggest that the moderate- to high-maturity crude oils correlate with immiscible oils in the main zone of oil generation from hydrous pyrolysis (330–360°C/72 hr). The preservation of distinct type I kerogens within the lacustrine depocenter is likely a consequence of variations in the organic source material (benthic vs. planktonic algae) and depositional environment (nearshore vs. offshore). This work documents these different open-lacustrine source facies and shows that the paraffinic crude oils in the Uinta basin originated from type I kerogen in source rocks such as the basal black shale facies.

Additional hydrous pyrolysis experiments on other units of the black shale facies further illustrate the variability of source rocks within the lacustrine system. In some instances, these samples appear to be correlated with other crude oils or pyrolysates in the literature. One sample of particular interest was an immiscible oil from the base of the carbonate marker, which appeared to have been generated from a source rock containing a mixture of the two end-member type I kerogens characterized in this investigation. This sample may represent a transition zone between the offshore open-lacustrine source facies (mahogany and upper carbonate marker) to more nearshore open-lacustrine source facies (lower black shale facies). These results show the importance of recognizing both vertical and lateral variability in source facies when undertaking oil–source rock correlation studies in lacustrine petroleum systems.

Stable carbon isotopic compositions of the gases produced by hydrous pyrolysis do not correlate with either group of natural gas samples previously analyzed from the Uinta basin. A progressive depth trend for methane $\delta^{13}C$ values among a group of Green River Formation natural gases from the Altamont field, however, suggests mixing of the natural gases with variable amounts of microbial gas. Correlation of ethane $\delta^{13}C$ values and the depth trends for methane $\delta^{13}C$ values suggests that nearshore open-lacustrine source rocks of the basal black shale facies are primarily responsible for the associated natural gas accumulations in Tertiary reservoirs in the Altamont field and possibly elsewhere in the Uinta basin.

Quantitative yields from Green River shale hydrous pyrolysis experiments were used to derive isothermal kinetic parameters for immiscible oil generation. Although the reaction mechanisms among the various organic phases are complex, the process of immiscible oil generation can be modeled as a pseudo–first-order reaction within a limited experimental range. An Arrhenius plot gives a linear expression (r = 0.98) that has an activation energy of 68.7 kcal/mol and a frequency factor of 1.65×10^{32} m.y.$^{-1}$ for combined data from both the mahogany shale and black shale facies. In contrast, kinetic parameters determined on aliquots of the same samples by nonisothermal open-system pyrolysis give much lower values for activation energies and frequency factors. This method results in a distribution of activation energies and a single frequency factor to describe the generation of hydrocarbons (bitumen + oil + gas) produced during Rock-Eval pyrolysis. For the mahogany shale there is a narrow distribution, where greater than 80% of the reactions have activation energies of about 51 kcal/mol, whereas the black shale facies source rock has a broader distribution between 46 and 52 kcal/mol.

Both sets of experimental kinetic parameters were used to model petroleum generation in the Altamont field along the northern margin of the Uinta basin. The results of these models indicate that hydrous pyrolysis kinetic parameters are more consistent with the observed natural data and offer a more coherent explanation for the extent and timing of oil generation in the Uinta basin. In the Rock-Eval kinetic model, hydrocarbon generation does not accurately match the proven zones of oil and gas production. The Rock-Eval model predicts that the basal Green River Formation is currently in the stage of wet-gas generation and that significant and active oil generation is occurring in the upper Green River Formation in stratigraphic horizons as shallow as the mahogany zone. These predictions are inconsistent with data that suggest the upper Green River source rocks are still immature with respect to oil generation and that the basal section is responsible for waxy oils that range from low to high maturity. In addition, predicted hydrocarbon generation occurs too early and too quickly in the Rock-Eval model to account for the overpressured reservoirs. As a consequence, the geothermal gradient and/or permeability input parameters in the Rock-Eval model must be lower than measured data to sustain overpressure. In contrast, the hydrous pyrolysis kinetic model accurately predicts that significant oil generation was restricted to the basal Green River source pod. Using the hydrous pyrolysis model, there is overlap in the predicted zone of oil generation, the measured zone of overpressure, and the location of a kink in the vitrinite reflectance profile. Transformation ratios in the basal Green River source pod range from 5 to 85% using hydrous pyrolysis kinetics. The remaining source potential predicted by this model suggests that active oil generation may account for overpressuring in the deeply buried Uinta basin reservoirs.

REFERENCES CITED

Abbott, W., 1957, Tertiary of the Uinta basin, *in* O. G. Seal, ed., Guidebook to the geology of the Uinta basin: Intermountain Association of Petroleum Geologists 8th Annual Field Conference Guidebook, p. 102–109.

Anders, D. E., and P. M. Gerrild, 1984, Hydrocarbon generation in lacustrine rocks of Tertiary age, Uinta basin, Utah—organic carbon, pyrolysis yield, and light hydrocarbons, *in* J. Woodward, F. F. Meissner, and J. L. Clayton, eds., Hydrocarbon source-rocks of the greater Rocky Mountain region: Denver, Rocky Mountain Association of Geologists, p. 513–523.

Anders, D. E., and W. E. Robinson, 1971, Cycloalkane constituents of the bitumens from the Green River shale: Geochimica et Cosmochimica Acta, v. 35, p. 661–678.

Anders, D. E., and W. E. Robinson, 1973, Geochemical aspects of the saturated hydrocarbon constituents of Green River oil shale—Colorado no. 1 core: U.S. Bureau of Mines Reports of Investigation 7737, 23 p.

Anders, D. E., F. G. Doolittle, and W. E. Robinson, 1975, Polar constituents isolated from Green River oil shale: Geochimica et Cosmochimica Acta, v. 39, p. 1423–1430.

Anders, D. E., J. G. Palacas, and R. C. Johnson, 1992, Thermal maturity of rocks and hydrocarbon deposits, Uinta basin, Utah, *in* T. D. Fouch, V. F. Nuccio, and T. C. Chidsey, eds., Hydrocarbon and mineral resources of the Uinta basin, Utah and Colorado: Utah Geological Association Guidebook 20, p. 53–76.

Baskin, D. K., and K. E. Peters, 1992, Early generation characteristics of a sulfur-rich Monterey kerogen: AAPG Bulletin, v. 76, p. 1–13.

Behar, F., M. Vandenbroucke, Y. Tang, F. Marquis, and J. Espitalie, 1997, Thermal cracking of kerogen in open and closed systems—determination of kinetic parameters and stoichiometric coefficients for oil and gas generation: Organic Geochemistry, v. 26, p. 321–339.

Bostick, N. H., J. R. Hatch, T. A. Daws, A. H. Love, C. M. Lubeck, and C. N. Threlkeld, 1987, Geological investigations of the Vermillion Creek coal bed in the Eocene Niland Tongue of the Wasatch Formation, Sweetwater County, Wyoming—organic geochemistry and organic petrography: U.S. Geological Survey Professional Paper 1314-H, p. 135–163.

Boyer, B. W., 1982, Green River laminites: does the playa-lake model really invalidate the stratified-lake model?: Geology, v. 10, p. 321–324.

Bradley, W. H., 1931, Origin and microfossils of the oil shale of the Green River Formation of Colorado and Utah: U.S. Geological Survey Professional Paper 168, 58 p.

Braun, R. L., and A. J. Rothman, 1975, Oil-shale pyrolysis—kinetics and mechanism of oil production: Fuel, v. 54, p. 129–131.

Bredehoeft, J. D., J. B. Wesley, and T. D. Fouch, 1994, Simulations of the origin of fluid pressure, fracture generation, and the movement of fluids in the Uinta basin, Utah: AAPG Bulletin, v. 78, p. 1729–1747.

Burger, J. A., 1963, The Cretaceous System of Utah, *in* A. L. Crawford, ed., The oil and gas possibilities of Utah, re-evaluated: Utah Geological and Mineralogical Survey Bulletin 54, paper 12, p. 123–140.

Burnham, A. K., R. L. Braun, and H. R. Gregg, 1987, Comparison of methods for measuring kerogen pyrolysis rates and fitting kinetic parameters: Energy and Fuels, v. 1, p. 452–458.

Burnham, A. K., R. L. Braun, and A. M. Samoun, 1988, Further comparison of methods for measuring kerogen pyrolysis rates and fitting kinetic parameters, *in* L. Mattavelli and L. Novelli, eds., Advances in organic geochemistry 1987: New York, Pergamon, p. 839–845.

Burnham, A. K., R. L. Braun, T. T. Coburn, E. I. Sandvik, D. J. Curry, B. J. Schmidt, and R. A. Noble, 1996, An appropriate kinetic model for well-preserved algal kerogens: Energy and Fuels, v. 10, p. 49–59.

Campbell, J. H., G. H. Koskinas, and N. D. Stout, 1978, Kinetics of oil generation from Colorado oil shale: Fuel, v. 57, p. 372–376.

Cashion, W. B., 1957, Stratigraphic relations and oil shale of the Green River Formation in the eastern Uinta basin, *in* O. G. Seal, ed., Guidebook to the geology of the Uinta basin: Intermountain Association of Petroleum Geologists 8th Annual Field Conference Guidebook, p. 131–135.

Cashion, W. B., and J. R. Donnell, 1974, Revision of the nomenclature of the upper part of the Green River Formation, Piceance Creek basin, Colorado, and eastern Uinta basin, Utah: U.S. Geological Survey Professional Paper 548, 48 p.

Castle, J. W., 1990, Sedimentation in Eocene Lake Uinta (lower Green River Formation), northeastern Uinta basin, Utah, *in* B. J. Katz, ed., Lacustrine basin exploration—case studies and modern analogs: AAPG Memoir 50, p. 243–263.

Cole, R. D., 1984, Sedimentological, mineralogical and geochemical definition of oil-shale facies in the lower Parachute Creek Member of the Green River Formation, Colorado, *in* J. H. Gary, ed., Proceedings of the 17th Oil Shale Symposium: Golden, Colorado, Colorado School of Mines Press, p. 143–158.

Cole, R. D., and M. D. Picard, 1978, Comparative mineralogy of nearshore and offshore lacustrine lithofacies, Parachute Creek Member of the Green River Formation, Piceance Creek basin, Colorado, and eastern Uinta basin, Utah: Geological Society of America Bulletin, v. 89, p. 1441–1454.

Cowardin, L. M., V. Carter, R. C. Golet, and E. T. LaRoe, 1979, Classification of wetlands and deepwater habitats of the United States: U.S. Fish and Wildlife Service, Biological Services Program FWS/PBS-79/31, 103 p.

Dane, C. H., 1954, Stratigraphic and facies relationships of upper part of Green River Formation and lower part of Uinta Formation in Duchesne, Uintah, and Wasatch counties, Utah: AAPG Bulletin, v. 38, p. 405–425.

Dane, C. H., 1955, Stratigraphic and facies relationships of the upper part of the Green River Formation and the lower part of the Uinta Formation in Duchesne, Uintah, and Wasatch counties, Utah: U.S. Geological Survey Oil and Gas Investigations Chart OC-52, 2 sheets.

Desborough, G. A., 1978, A biogenic-chemical stratified lake model for the origin of oil shale of the Green River Formation—an alternative to the playa-lake model: Geological Society of America Bulletin, v. 89, p. 961–971.

Dyni, J. R., C. Milton, and W. R. Cashion, 1985, The saline facies of the upper part of the Green River Formation near Duchesne, Utah, *in* M. D. Picard, ed., Geology and energy resources, Uinta basin of Utah: Utah Geological Association Publication 12, p. 51–60.

Eglinton, T. I., A. G. Douglas, and S. J. Rowland, 1988, Release of aliphatic, aromatic and sulphur compounds from Kimmeridge kerogen by hydrous pyrolysis—a quantitative study, *in* L. Mattavelli and L. Novelli, eds., Advances in organic geochemistry 1987: New York, Pergamon, p. 655–663.

Eugster, H. P., and L. A. Hardie, 1975, Sedimentation in an ancient playa-lake complex—the Wilkins Peak Member of the Green River Formation of Wyoming: Geological Society of America Bulletin, v. 86, p. 319–334.

Eugster, H. P., and R. C. Surdam, 1973, Depositional environment of the Green River Formation of Wyoming—a preliminary report: Geological Society of America Bulletin, v. 84, p. 1115–1120.

Evans, R. J., and G. T. Felbeck Jr., 1983, High temperature simulation of petroleum formation—I. the pyrolysis of Green River shale: Organic Geochemistry, v. 4, p. 135–144.

Fouch, T. D., 1975, Lithofacies and related hydrocarbon accumulations in Tertiary strata of the western and central Uinta basin, Utah, *in* D. W. Bolyard, ed., Deep drilling frontiers of the central Rocky Mountains: Denver, Rocky Mountain Association of Geologists Symposium, p. 163–174.

Fouch, T. D., 1976, Revision of the lower part of the Tertiary System in the central and western Uinta basin, Utah: U.S. Geological Survey Bulletin 1405-C, p. C1–C7.

Fouch, T. D., 1981, Distribution of rock types, lithologic groups, and interpreted depositional environments for some lower Tertiary and Upper Cretaceous rocks from outcrops at Willow Creek–Indian Canyon through the subsurface of Duchesne and Altamont oil fields, southwest to north central parts of the Uinta basin, Utah: U.S. Geological Survey Oil and Gas Investigations Chart OC-81, 2 sheets.

Fouch, T. D., W. B. Cashion, R. T. Ryder, and J. A. Campbell, 1976, Field guide to lacustrine and related nonmarine depositional environments in Tertiary rocks, Uinta basin, Utah, *in* R. C. Epis and R. J. Weimer, eds., Studies in Colorado field geology: Professional Contributions of Colorado School of Mines 8, p. 358–385.

Fouch, T. D., G. E. Claypool, J. H. Hanley, and R. H. Tschudy, 1977, Newly recognized petroleum source-rock units in east-central Utah—implications for detection of petroleum in nonmarine units (abs.): AAPG Bulletin, v. 61, p. 785–786.

Fouch, T. D., V. F. Nuccio, J. C. Osmond, L. MacMillan, W. B. Cashion, and C. J. Wandrey, 1992, Oil and gas in uppermost Cretaceous and Tertiary rock, Uinta basin, Utah, *in* T. D. Fouch, V. F. Nuccio, and T. C. Chidsey, eds., Hydrocarbon and mineral resources of the Uinta basin, Utah and Colorado: Utah Geological Association Guidebook 20, p. 9–47.

Fouch, T. D., V. F. Nuccio, D. E. Anders, D. D. Rice, J. K. Pitman, and R. F. Mast, 1994, Green River (!) petroleum system, Uinta basin, Utah, U.S.A., *in* L. B. Magoon and W. G. Dow, eds., The petroleum system—from source to trap: AAPG Memoir 60, p. 399–421.

Franczyk, K. J., J. K. Pitman, W. B. Cashion, J. R. Dyni, T. D. Fouch, R. C. Johnson, M. A. Chan, J. R. Donnell, T. F. Lawton, and R. R. Remy, 1989, Evolution of resource-rich foreland and intermontane basins in eastern Utah and western Colorado: 28th International Geological Congress Field Trip Guidebook T-324, American Geophysical Union, 53 p.

Hanley, J. H., 1976, Paleosynecology of nonmarine Mollusca from the Green River and Wasatch formations (Eocene), southwestern Wyoming and northwestern Colorado, *in* R. W. Scott and R. R. West, eds., Structure and classification of paleocommunities: Stroudsburg, Pennsylvania, Dowden, Hutchinson and Ross, p. 235–261.

Hanley, J. H., T. D. Fouch, G. E. Claypool, and R. H. Tschudy, 1976, Palentology, geochemistry, and depositional environments of some lower Tertiary coals, north-central Utah—implications for detection of contential petroleum source-rocks (abs.): Annual Meeting of the Geological Society of America Abstracts with Program, p. 902.

Hatcher, H. J., H. L. C. Meuselaar, and D. T. Urban, 1992, A comparison of biomarkers in gilsonite, oil shale, tar sand and petroleum from Threemile Canyon and adjacent areas in the Uinta basin, Utah, *in* T. D. Fouch, V. F. Nuccio, and T. C. Chidsey, eds., Hydrocarbon and mineral resources of the Uinta basin, Utah and Colorado: Utah Geological Association Guidebook 20, p. 271–287.

Horsfield, B., et al., 1994, Organic geochemistry of freshwater and alkaline lacustrine sediments in the Green River Formation of the Washakie basin, Wyoming, U.S.A., *in* N. Telnæs et al., eds., Advances in organic geochemistry 1993: New York, Pergamon, p. 415–440.

Huizinga, B. J., Z. A. Aizenshtat, and K. E. Peters, 1988, Programmed pyrolysis–gas chromatography of artificially matured Green River kerogen: Energy and Fuels, v. 2, p. 74–81.

Hunt, J. M., 1963, Composition and origin of the Uinta basin bitumens, *in* A. L. Crawford, ed., The oil and gas possibilities of Utah, re-evaluated: Utah Geological and Mineralogical Survey Bulletin 54, paper 24, p. 249–273.

Hunt, J. M., 1979, Petroleum geochemistry and geology: San Francisco, W. H. Freeman and Company, 617 p.

Hunt, J. M., M. D. Lewan, and R. J-C. Hennet, 1991, Modeling oil generation with time-temperature index graphs based on the Arrhenius equation: AAPG Bulletin, v. 75, p. 795–807.

Hutton, A. C., 1988, North American oil shales, *in* Organic petrography of oil shales: U.S. Geological Survey Short Course Notes, p. 230–264.

Johnson, R. C., 1985, Early Cenozoic history of the Uinta and Piceance Creek basins, Utah and Colorado, with special reference to the development of Eocene Lake Uinta, *in* M. Flores and S. S. Kaplan, eds., Cenozoic paleogeography of west-central United States: Rocky Mountain Section SEPM Symposium, p. 247–276.

Jones, D. M., A. G. Douglas, and J. Connan, 1988, Hydrous pyrolysis of asphaltenes and polar fractions of biodegraded oils, *in* L. Mattavelli and L. Novelli, eds., Advances in organic geochemistry 1987: New York, Pergamon, p. 981–993.

Katz, B. J., and L. Xingcai, 1998, Summary of the AAPG Research Symposium on lacustrine basin exploration in China and southeast Asia: AAPG Bulletin, v. 82, p. 1300–1307.

Law, B. E., V. F. Nuccio, and C. E. Barker, 1989, Kinky vitrinite reflectance profiles—evidence of paleopore pressures in low-permeability, gas-bearing sequences in the Rocky Mountain foreland basins: AAPG Bulletin, v. 73, p. 999–1010.

Leavitt, D. R., A. L. Tyler, and A. S. Kafesjian, 1987, Kerogen decomposition kinetics of selected Green River and eastern U.S. oil shales from thermal solution experiments: Energy and Fuels, v. 1, p. 520–525.

Leopold, E. B., 1969, Late Cenozoic palynology, *in* R. H. Tschudy and R. A. Scott, eds., Aspects of palynology: New York, Wiley-Interscience, p. 377–438.

Lewan, M. D., 1985, Evaluation of petroleum generation by hydrous pyrolysis experimentation: Philosophical Transactions of the Royal Society London, Series A 315, p. 123–134.

Lewan, M. D., 1991, Primary oil migration and expulsion as determined by hydrous pyrolysis: Proceedings of the 13th World Petroleum Congress, no. 2, p. 215–223.

Lewan, M. D., 1992, A concise historical and current perspective on the kinetics of natural oil generation, *in* L. B. Magoon, ed., The petroleum system—status of research and methods, 1992: U.S. Geological Survey Bulletin 2007, p. 12–15.

Lewan, M. D., 1993, Laboratory simulation of petroleum formation—hydrous pyrolysis, *in* M. H. Engel and S. A. Macko, eds., Organic geochemistry, principles and applications: New York, Plenum, p. 419–444.

Lewan, M. D., 1994, Assessing natural oil expulsion from source-rocks by laboratory pyrolysis, *in* L. B. Magoon and W. G. Dow, eds., The petroleum system—from source to trap: AAPG Memoir 60, p. 201–210.

Lewan, M. D., 1997, Experiments on the role of water in petroleum formation: Geochimica et Cosmochimica Acta, v. 61, p. 3691–3723.

Lewan, M. D., 1998, Reply to the comment by A. K. Burnham on "experiments on the role of water in petroleum formation": Geochimica et Cosmochimica Acta, v. 62, p. 2211–2216.

Lewan, M. D., J. C. Winters, and J. H. McDonald, 1979, Generation of oil-like pyrolyzates from organic-rich shales: Science, v. 203, p. 897–899.

Lucas, P. T., and J. M. Drexler, 1975, Altamont-Bluebell—a major fractured and overpressured stratigraphic trap, Uinta basin, Utah, *in* D. W. Bolyard, ed., Deep drilling frontiers of the central Rocky Mountains: Denver, Rocky Mountain Association of Geologists Symposium, p. 265–273.

McPherson, B. J. O. L., 1996, A three-dimensional model of the geological and hydrodynamic history of the Uinta basin, Utah—analysis of overpressures and oil migration: Ph.D. dissertation, University of Utah, Salt Lake City, Utah, 119 p.

Michels, R., and P. Landais, 1994, Artificial coalification—comparison of confined pyrolysis and hydrous pyrolysis: Fuel, v. 73, p. 1691–1696.

Montgomery, S. L., and C. D. Morgan, 1998, Bluebell field, Uinta basin—reservoir characterization for improved well completion and oil recovery: AAPG Bulletin, v. 82, p. 1113–1132.

Mueller, E., 1998, Temporal and spatial source rock variations and the effects on crude oil composition and hydrocarbon generation in the Tertiary petroleum system of the Uinta basin, Utah, U.S.A.: Ph.D. dissertation, University of Oklahoma, Norman, Oklahoma, 170 p.

Nichols, D. J., 1987, Geological investigations of the Vermillion Creek coal bed in the Eocene Niland Tongue of the Wasatch Formation, Sweetwater County, Wyoming—palynology of the Vermillion Creek coal bed and associated strata: U.S. Geological Survey Professional Paper 1314-D, p. 49–73.

Osmond, J. C., 1964, Tectonic history of the Uinta basin, Utah, *in* E. F. Sabatka, ed., Guidebook to the geology and mineral resources of the Uinta basin: Intermountain Association of Petroleum Geologists 13th Annual Field Conference Guidebook, p. 47–58.

Pepper, A. S., 1991, Estimating the petroleum expulsion behaviour of source rocks—a novel quantitative approach, *in* W. A. England and A. J. Fleet, eds., Petroleum migration: London, Geological Society Special Publication 59, p. 9–31.

Peters, K. E., and J. M. Moldowan, 1993, The biomarker guide—interpreting molecular fossils in petroleum and ancient sediments: Englewood Cliffs, New Jersey, Prentice-Hall, 363 p.

Peters, K. E., J. M. Moldowan, and P. Sundararaman, 1990, Effects of hydrous pyrolysis on biomarker thermal maturity parameters—Monterey Phosphatic and Siliceous members: Organic Geochemistry, v. 15, p. 249–265.

Philippi, G. T., 1974, The influence of marine and terrestrial source material on the composition of petroleum: Geochimica et Cosmochimica Acta, v. 38, p. 947–966.

Philp, R. P., A. N. Bishop, J. C. Del Rio, and J. Allen, 1995, Characterization of high molecular weight hydrocarbons ($>C_{40}$) in oils and reservoir rocks, *in* J. M. Cubitt and W. A. England, eds., The geochemistry of reservoirs: London, Geological Society Special Publication 86, p. 71–85.

Picard, M. D., 1955, Subsurface stratigraphy and lithology of Green River Formation in Uinta basin, Utah: AAPG Bulletin, v. 39, p. 75–102.

Picard, M. D., 1957, Green River and lower Uinta Formation subsurface stratigraphy in central and eastern Uinta basin, Utah, *in* O. G. Seal, ed., Guidebook to the geology of the Uinta basin: Intermountain Association of Petroleum Geologists 8th Annual Field Conference Guidebook, p. 116–130.

Picard, M. D., 1959, Green River and lower Uinta Formation subsurface stratigraphy in western Uinta basin, Utah, *in* N. C. Williams, ed., Guidebook to the geology of the Wasatch and Uinta Mountains transition area: Intermountain Association of Petroleum Geologists 10th Annual Field Conference Guidebook, p. 139–149.

Picard, M. D., 1985, Hypothesis of oil-shale genesis, Green River Formation, northeast Utah, northwest Colorado, and southwest Wyoming, *in* M. D. Picard, ed., Geology and energy resources, Uinta basin of Utah: Utah Geological Association Publication 12, p. 193–210.

Picard, M. D., W. D. Thompson, and C. R. Williamson, 1973, Petrology, geochemistry and stratigraphy of black shale facies of Green River Formation (Eocene), Uinta basin, Utah: Utah Geological and Mineralogical Survey Bulletin 100, 52 p.

Porter, L., 1963, Stratigraphy and oil possibilities of the Green River Formation in the Uinta basin, Utah, *in* A. L. Crawford, ed., The oil and gas possibilities of Utah, re-evaluated: Utah Geological and Mineralogical Survey Bulletin 54, paper 19, p. 193–198.

Qiang, J., and P. J., McCabe, 1998, Genetic features of petroleum

systems in rift basins of eastern China: Marine and Petroleum Geology, v. 15, p. 343–358.

Qiang, J., W. Weifeng, X. Huaimin, Y. Shaochun, and Q. Ji, 1997, North Jiangsu basin, eastern China—accumulation of immature oils and diagenesis of Palaeogene reservoir rocks: Journal of Petroleum Geology, v. 20, p. 287–306.

Ray, R. G., B. H. Kent, and C. H. Dane, 1956, Stratigraphy and photogeology of the southwestern part of the Uinta basin Duchesne and Uintah counties, Utah: U.S. Geological Survey Oil and Gas Investigations Map OM-171, scale 1:63,360, 2 sheets.

Reed, W. E., and W. Henderson, 1972, Proposed stratigraphic controls on the composition of crude oils reservoired in the Green River Formation, Uinta basin, Utah, *in* H. R. Gaertner and H. Wehner, eds., Advances in organic geochemistry 1971: New York, Pergamon, p. 499–515.

Remy, R. R., 1992, Stratigraphy of the Eocene part of the Green River Formation in the south-central part of the Uinta basin, Utah: U.S. Geological Survey Bulletin 1787, p. BB1–BB25.

Rice, D. D., T. D. Fouch, and R. C. Johnson, 1992, Influence of source-rock type, thermal maturity, and migration on composition and distribution of natural gases, Uinta basin, Utah, *in* T. D. Fouch, V. F. Nuccio, and T. C. Chidsey, eds., Hydrocarbon and mineral resources of the Uinta basin, Utah and Colorado: Utah Geological Association Guidebook 20, p. 95–109.

Robbins, E. I., 1987, Geological investigations of the Vermillion Creek coal bed in the Eocene Niland Tongue of the Wasatch Formation, Sweetwater County, Wyoming—paleocology of the Niland Tongue: U.S. Geological Survey Professional Paper 1314-E, p. 77–103.

Robinson, W. E., 1969, Kerogen of the Green River Formation, *in* G. Eglinton and M. T. J. Murphy, eds., Organic geochemistry—methods and results: New York, Springer-Verlag, p. 619–637.

Robinson, W. E., and G. L. Cook, 1975, Compositional variations of organic material from Green River oil shale—WOSCO EX-1 core (Utah): U.S. Bureau of Mines Reports of Investigation 8017, 40 p.

Robinson, W. E., J. J. Cummins, and G. U. Dinneen, 1965, Changes in Green River oil-shale paraffins with depth: Geochimica et Cosmochimica Acta, v. 29, p. 249–258.

Ruble, T. E., 1990, Organic geochemical investigation of native bitumens from the Uinta basin, Utah, U.S.A.: M.S. thesis, University of Oklahoma, Norman, Oklahoma, 155 p.

Ruble, T. E., 1996, Geochemical investigation of the mechanisms of hydrocarbon generation and accumulation in the Uinta basin, Utah: Ph.D. dissertation, University of Oklahoma, Norman, Oklahoma, 333 p.

Ruble, T. E., and R. P. Philp, 1998, Stratigraphy, depositional environments and organic geochemistry of source-rocks in the Green River petroleum system, Uinta basin, Utah, *in* J. K. Pitman and A. R. Carroll, eds., Modern and ancient lake systems—new problems and perspectives: Utah Geological Association Guidebook 26, p. 289–328.

Ryder, R. T., T. D. Fouch, and J. H. Elison, 1976, Early Tertiary sedimentation in the western Uinta basin, Utah: Geological Society of America Bulletin, v. 87, p. 496–512.

Schenk, H. J., B. Horsfield, B. Krooss, R. G. Schaefer, and K. Schwochau, 1997, Kinetics of petroleum formation and cracking, *in* D. H. Welte, B. Horsfield, and D. R. Baker, eds., Petroleum and basin evolution—insights from petroleum geochemistry, geology and basin modeling: New York, Springer-Verlag, p. 231–269.

Shih, S. M., and H. Y. Sohn, 1980, Nonisothermal determination of the intrinsic kinetics of oil generation from oil shale: Industrial and Engineering Chemistry—Process Design and Development, v. 19, p. 420–426.

Snowdon, L. R., 1979, Errors in extrapolation of experimental kinetic parameters to organic geochemical systems: AAPG Bulletin, v. 63, p. 1128–1138.

Stanton, R. W., J. A. Minkin, and T. A. Moore, 1987, Geological investigations of the Vermillion Creek coal bed in the Eocene Niland Tongue of the Wasatch Formation, Sweetwater County, Wyoming—petrographic and physical properties of coal and rock samples: U.S. Geological Survey Professional Paper 1314-F, p. 107–120.

Surdam, R. C., and C. A. Wolfbauer, 1975, Green River Formation, Wyoming—a playa-lake complex: Geological Society of America Bulletin, v. 86, p. 335–345.

Sweeney, J. J., 1988, Application of maturation indicators and oil reaction kinetics to put constraints on thermal history models for the Uinta basin, Utah, U.S.A., *in* L. Mattavelli and L. Novelli, eds., Advances in organic geochemistry 1987: New York, Pergamon, p. 199–205.

Sweeney, J. J., A. K. Burnham, and R. L. Braun, 1987, A model of hydrocarbon generation from type I kerogen—application to Uinta basin, Utah: AAPG Bulletin, v. 71, p. 967–985.

Tissot, B., and D. H. Welte, 1978, Petroleum formation and occurrence—a new approach to oil and gas exploration: New York, Springer-Verlag, 538 p.

Tissot, B., G. Deroo, and A. Hood, 1978, Geochemical study of the Uinta basin—formation of petroleum from the Green River Formation: Geochimica et Cosmochimica Acta, v. 42, p. 1469–1485.

Untermann, G. E., and B. R. Untermann, 1968, Geology of Uintah County: Utah Geological and Mineralogical Survey Bulletin 72, 98 p.

Walther, J., 1894, Einleitung in die Geologie als historische Wissenschaft—Lithogenesis der Gegenwart, v. 3: Jena, Germany, Fischer Verlag, p. 535–1055.

Waples, D. W., 1984, Thermal models of oil generation, *in* J. Brooks and D. H. Welte, eds., Advances in petroleum geochemistry, v. I: London, Academic Press, London, p. 7–68.

Weiss, M. P., I. J. Witkind, and W. B. Cashion, 1990, Geologic map of the Price 30′ × 60′ quadrangle, Carbon, Duchesne, Uintah, Utah, and Watsatch counties, Utah: U.S. Geological Survey Miscellaneous Investigations Series Map I-1981, scale 1:100,000, 1 sheet.

Wesley, J. B., 1990, Finite difference modeling of present-day overpressures maintained by hydrocarbon generation, and regional fluid flow in the Green River Formation of the Uinta basin: M.S. thesis, Colorado School of Mines, Golden, Colorado, 139 p.

Whiticar, M. J., 1994, Correlation of natural gases with their sources, *in* L. B. Magoon and W. G. Dow, eds., The petroleum system—from source to trap: AAPG Memoir 60, p. 261–283.

Wiggins, W. D., and P. M. Harris, 1994, Lithofacies, depositional cycles, and stratigraphy of the lower Green River Formation, southwestern Uinta basin, Utah: Notes for SEPM Core Workshop—Lacustrine Source-rock Depositional Environments, AAPG Annual Meeting, 22 p.

Williamson, C. R., and M. D. Picard, 1974, Petrology of carbonate rocks of the Green River Formation (Eocene): Journal of Sedimentary Petrology, v. 44, p. 738–759.